FINAL TECHNICAL REPORT
NASA GRANT 5-834

INVESTIGATION OF THERMAL-FLUID MECHANICAL CHARACTERISTICS OF THE CAPILLARY PUMP LOOP

By

Ali M. Kiper

School of Engineering and Applied Science
The George Washington University
Washington, DC 20052

Submitted to

National Aeronautics and Space Administration
Goddard Space Flight Center
Greenbelt, Maryland 20771

NASA Technical Officer
Theodore D. Swanson
Code 732

August 1991

Table of Contents

7. CONCLUSIONS AND RECOMMENDATIONS

List of Figures

List of Figures - cont'd...

List of Tables

INVESTIGATION OF THERMAL-FLUID MECHANICAL CHARACTERISTICS OF THE CAPILLARY PUMP LOOP

1. INTRODUCTION

Temperature control of large space structures, such as Space Station will require advanced heat acquisition and transport system to keep on-board temperatures within their allowable ranges. Two-phase temperature control system which utilizes an evaporation-condensation cycle offer significant advantage for such applications. The Capillary Pumped Loop (CPL) heat pipe is such a two-phase heat transport system which utilizes the surface tension forces developed in a fine pore capillary wick to circulate the working fluid.

The CPL test system has exhibited up to an 8 kw heat load capacity over 10 meter transport distance in one-g environment [1]. Recent testing of the High Power Spacecraft Thermal Management (HPSTM) demonstration system has shown that in the capillary mode, the HPSTM evaporators can acquire a total heat load of between 600 W and 24 kw [1]. Testing of a small-scale CPL experiment aboard Space Shuttle verified the thermal control capability of this system in a microgravity environment.

A CPL assembly which is integrated into a system such as a spacecraft is expected to perform in a wide range of thermal environment of space. Therefore, an analyst may need to simulate and evaluate the operation of the CPL system under transient conditions. Although, recently, a computer model was developed to predict the steady state and transient behavior of a CPL heat pipe, there exists a need for both test data of the transient CPL operation, as well as a reasonable simple CPL model which can be used for evaluating this data [2]. Such a model would allow direct study of pertinent system parameters on the transient CPL heat pipe operation.

The actual CPL system in a space station structure will definitely undergo transient operations of various kinds. It is, therefore, important that one should understand the transient characteristics of the CPL heat pipe. If, one could ensure that the transient system would move from one steady state to another, there would be no operational complication. However, during such a transition, the instability could occur, leading to a rapid performance deterioration. For this reason, a complete understanding of transient instability characteristics of the CPL System is needed in order to ensure a reliable system operation.

Although transient operation of the conventional heat pipes subjected to various external operating conditions has been studied, such investigations have not dealt with the instability considerations. Furthermore, information on transient behavior of the loop-type heat pipes is either unavailable, or incomplete.

The available CPL test data seems to indicate that the low temperature transient characteristics of this system is similar, in many ways, to that of more conventional two phase flow systems. Therefore, it is expected that the results and the methods available in the two-phase flow literature can be used to investigate the transient CPL behavior. Many two-phase flow systems are susceptible to thermal-hydrodynamic instabilities, which may cause flow excursions, or flow oscillations of constant amplitude, or diverging amplitude. These excursions and oscillations could induce boiling crisis, disturb control system, or cause mechanical damage. Knowledge of the existence, and prediction of the threshold of instability in a two-phase flow system, therefore, is very important in order to avoid the instability conditions, or to compensate for it.

The foregoing brief introduction is believed to indicate that a better understnding of thermo-fluid mechanic characteristics of the CPL system requires study of transient

behavior of this system under different conditions.

An instability in a heated fluid channel, or in a two-phase flow system can be a primary or secondary phenomenon. It can be static, or dynamic in nature. A flow is subjected to a "static instability" if, when the flow conditions change by a small step from the original steady state ones, another steady state is not possible in the vicinity of the original state. The cause of the phenonmenon lies in the steady state laws; hence, the threshold of the instability can be predicted only by using steady state laws. A static instability can lead either to a different steady state condition, or to a periodic behavior.

A flow is subject to a "dynamic instability" when the inertia and other feedback effects have an essential part in the process. The system behaves like a servomechanism, and the knowledge of the steady state laws is not sufficient, even for threshold prediction. An instability is "compound" when several elementary mechanisms interact in the process and cannot be studied separately. Density wave oscillations are perhaps the most frequently observed and analyzed dynamic instabilities.

Two examples to compound dynamic instability are (i) "thermal oscillation," caused by interaction of variable heat transfer coefficient with flow dynamics, and (ii) "Parallel channel instability," caused by interaction among small number of parallel channels. Both of these instability conditions could be involved in the CPL transient operation. Compared with the conventional heat pipes, loop arrangement of the CPL System is susceptible to dynamic feedback effects that may lead to flow and temperature oscillations. Possibility of incipience of nucleation at the CPL evaporator inlet, and existence of non-condensible gases may vary significantly the convective heat transfer coefficient, and could cause thermal oscillations at the evaporator inlet.

In fact, in some test runs of the NASA/GSFC (Goddard Space Flight Center) CPL-2 system, a step change in power input to evaporators was accompanied by low frequency temperature oscillations at the evaporator inlet section.

Assessment of the available CPL test data indicated a need for in-depth study of the transient thermal-fluid mechanic processes occurring in different parts of the CPL system. Of particular interest is the explanation of the aforesaid temperature oscillations. Although several theories have been forwarded to explain this observed phenomenon, a satisfactory understanding of these temperature fluctuations

is still lacking. It is well known that, Ref. [3], thermally induced oscillations can introduce operational problems in two-phase flow systems, such as the CPL system, if they lead to flow or temperature instabilities. Therefore, the reliable operation of the CPL system necessitates understanding of characteristics of the observed temperature fluctuations, as well as the conditions of stability of such transient phenomena.

2. PROGRAM WORK

The main purpose of the present program work is the experimental and analytical study of behavior of the CPL heat pipe system during the transient mode of operation by applying a step heat pulse to one or more evaporators. Prediction of the CPL behavior when subjected to pulse heat loading requires further study before the transient response of CPL system can be fully understood. Two important questions that require answers are:

(i) After a suddenly applied pulse heat load, will a CPL heat pipe maintain normal operation? If so, how large may this load be?

(ii) Are there operational conditions which may cause unstable CPL behavior?

In the present study, these questions are investigated experimentally and simple theoretical models are used to explain some characteristics of the transient CPL operation. The program work consists of the following tasks:

- Exploratory testing of a NASA/GSFC CPL heat pipe for transient operational conditions which could generate the type of oscillatory inlet temperature behavior observed in an earlier testing of NASA/GSFC CPL- 2 heat pipe system.

- Analytical investigation of the CPL inlet section temperature oscillations.

- Design, construction and testing of a bench-top CPL test system for study of the CPL transient operation.

- Transient analysis of a CPL heat pipe by applying a step power input to the evaporators.

Program activities undertaken in each project task, as well as results obtained, have been presented and discussed in following sections of the present report.

3. TEST OF NASA/GSFC CPL HEAT PIPE

For the purpose of investigating the operational conditions which could lead to the mentioned oscillatory temperature behavior, a CPL test system was obtained from NASA/GSFC on a loan basis and placed in the School of Engineering Heat Transfer Laboratory.

A layout of the CPL test system is shown in Fig. 1. The system uses Freon 11 as the working fluid. It incorporates two capillary pump evaporators, liquid and vapor transport lines, a condensing cold plate, a liquid sub-cooler, a reservoir, liquid isolators and evaporator inlet sub-coolers. A mechanical pump was also incorporated in the CPL system. Although this pump had been used in an earlier test program to evaluate the hybrid capillary/mechanically pumped system behavior, it was not used in our test runs.

Construction of the CPL evaporator consists of an axially grooved tubing outer shell and an internal wick structure made of high density polyethylene porous material. Thermocouple locations of the test system (38 thermocouples) are shown in Fig. 1. Other details of the CPL test loop is given in Refs. [4, 5]. Auxiliary equipment and computerized data acquisition system used in this testing task is the same as that used in the second experimental task of the present investigation.

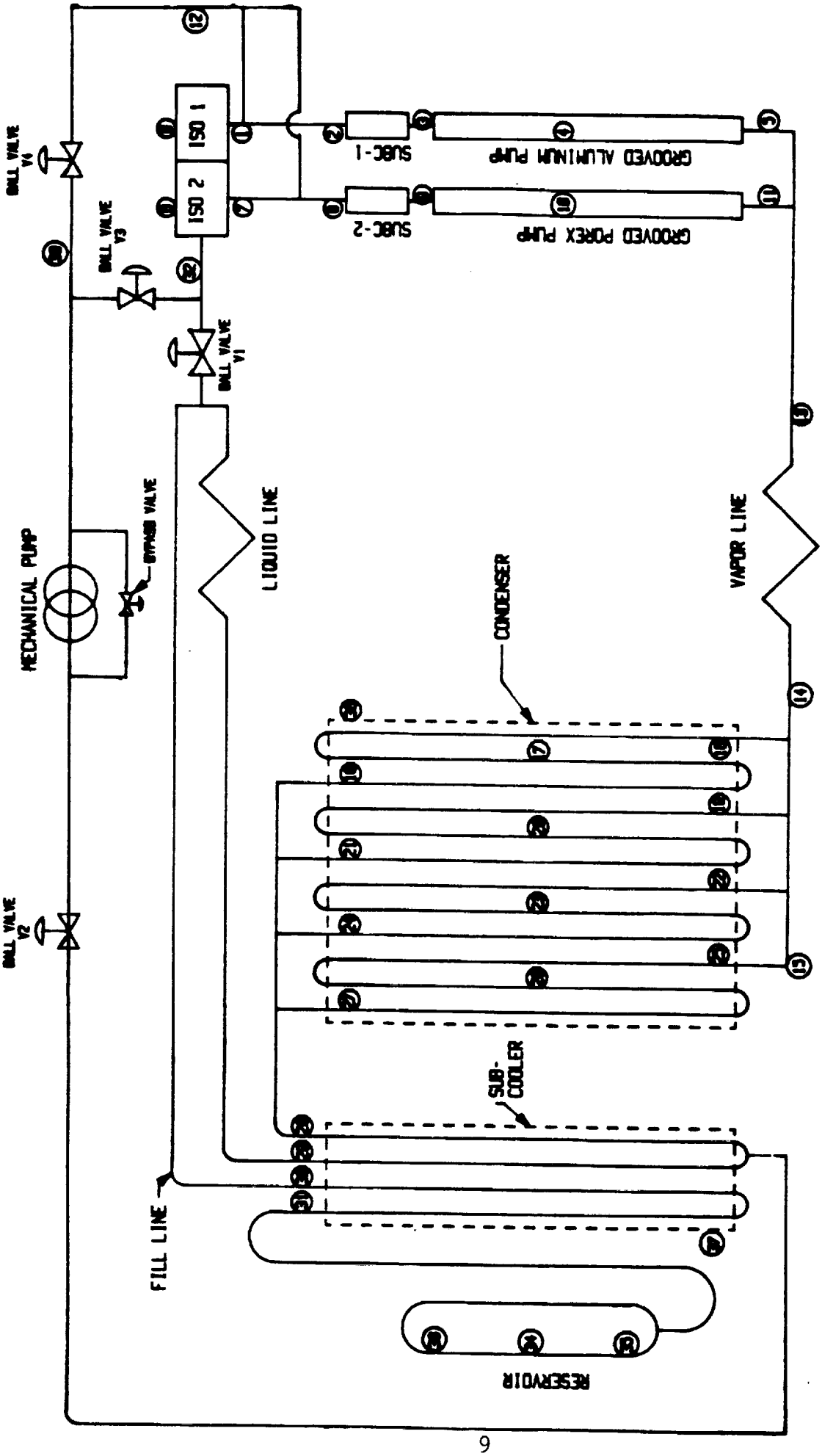

ORIGINAL PAGE IS
OF POOR QUALITY

Therefore, information on these items is given in Sec. 5 of this report.

Following the standard test system preparations and the start-up procedures, the CPL system was tested. During the first several days of testing, it was determined that additional sub-cooling of incoming liquid was required. Although the cold plate included a sub-cooling pass, under low flow conditions, parasitic heat gains significantly reduced or even eliminated the sub-cooling. To improve this condition, some part of the chiller liquid was circulated through the evaporator inlet subcoolers. With proper inlet subcooling, system start-ups were successful.

During several days of testing, many test runs were performed by applying step heat pulses of the same magnitude to each of two evaporators. Transient temperature variations, especially at evaporator inlet locations were, monitored and recorded. Tests were repeated at different loop operating temperatures by varying the reservoir temperature. This temperature was manually controlled by changing the heat input to the reservoir.

As mentioned earlier, purpose of these tests were to explore possible operating conditions which could produce oscillatory temperature behavior at the evaporator inlet

section. As it turned out, performance of the test CPL system during the testing period was rather predictable. No unusual transient behavior was displayed similar to the temperature oscillations which had appeared in the evaporator inlet lines of the NASA/GSFC CPL-2 test system in the earlier testing program. Efforts to produce such temperature oscillations were not successful. Transient temperature changes between steady states took place without any noticeable oscillatory behavior. At low and close to dry-out power inputs, however, reproduction of the test data under apparently similar operational conditions were not very consistent, indicating possible additional factors effecting the transient behavior under limiting power inputs.

Critical evaluations of the experimental test data obtained from CPL-2 and the other NASA/GSFC CPL systems, including the one discussed here, seem to indicate that anomalies in the transient behavior, such as oscillatory temperature, are design-oriented rather than operation-oriented. The term 'anomaly' is used here to describe an unexpected behavior. Otherwise, although the transient CPL behavior at low power limit and dry-out may be considered as anomalies in the transient behavior, yet, they are expected.

On the basis of results of this task activity, one may tentatively conclude that with proper CPL design oscillatory transient behavior can be prevented. The analytical study given in Appendix A identifies the relevant design parameters and presents a criterion that can be used to predict conditions which may cause the oscillatory transient CPL behavior. Further study is needed for better understanding of this transient phenomenon.

4. ANALYTICAL INVESTIGATION OF THE CPL INLET SECTION TEMPERATURE OSCILLATIONS

In this task, an analytical study has been conducted for better understanding of a peculiar transient behavior which was displayed in earlier testing of the NASA/GSFC CPL-2 test heat pipe system. During several test runs of this system, varying degrees of surface temperature oscillations had occurred in the inlet line of the evaporators. Although several theories have been forwarded to explain this observed phenomenon, a satisfactory understanding of the cause of these temperature oscillations is still missing.

The present analytical work describes the conditions which lead to such oscillatory temperature behavior in evaporator inlet section of a CPL heat pipe. Details of this

study is given in Appendix A. Here, only some of the results and conclusions will be summarized. In this study, a solution is obtained representing the conditions which would cause an oscillating contribution to the transient wall temperture variation in the inlet section of the CPL evaporators. Stability characteristics of these temperature oscillations were investigated and a preliminary stability criterion was introduced.

When a step power input is applied to evaporator of a given CPL heat pipe, under stable operation, the system will move to a different steady state. Referring to Relation (39) in Appendix A, so long as magnitude of the heat flow to evaporator at the new steady state remained below a critical value, the CPL inlet pipe and evaporator wall temperatures will not include any oscillatory terms.

Relation (39) implies that at a given steady state heat input, evaporator inlet sections having large diameters and wall thickness and made of materials of high thermal conductivities, are better for preventing the temperature oscillations. The same is true for large values of convective heat transfer coefficient between the working fluid and the inlet pipe wall. For this reason, a significant decrease in the convective heat transfer coefficient caused by liquid bubbling or accumulation of non-condensible gases in

the inlet section could lead to temperature oscillations.

Therefore, the inlet section design of the NASA/GSFC CPL-2 test section with its stainless steel piping and a multi-component brazing section would enhance occurrence of wall temperature oscillations. The situation is aggravated at low heat inputs since, the low liquid flow rate helps initiation of boiling and non-condensible gas accumulation at the evaporator inlet section. Relation (39) also indicates that increased inlet sub-cooling would help to prevent the oscillatory temperature contributions.

In Appendix A, predictions of the present analytical investigation are compared with some test data obtained earlier during testing of the CPL-2 heat pipe system. Agreement between the predictions and the experimental temperature oscillation data was found to be reasonably good. However, it is important to emphasize that this problem requires further study.

NEED FOR THE BENCH-TOP CPL SYSTEM

A critical reveiw of conditions of the CPL operation, as well as the CPL test data, has revealed the fact that for a better understanding of characteristics of the CPL transient behavior, account must be taken of the internal fluid dynamic

parameters. This can be facilitated by using a reasonably simple test system which would allow visual observations of the possible formation of non-condensible gas or vapor bubbles, and the distribution of liquid flow under steady and transient operations. For this purpose, a bench-top CPL system has been designed and fabricated.

This test system is used to investigate the transient heat pipe performance. The transient behavior is studied by visual observations under varying test conditions, and the data collected is evaluated for better understanding of the process characteristics. Design of the bench-top system allows easy variation of most of the parameters controlling the transient heat pipe performance, as well as the internal visual observation of the CPL operation.

5. TEST OF BENCH-TOP CPL SYSTEM

5.1 Description of the Test System

A schematic of the bench-type rig is presented in Fig. 2. The system incorporates four evaporator chambers, reservoir, condenser, vacuum pump, temperature sensors and other instrumentation and Data Acquisition and Control System. The Capillary Pumped Loop test system uses distilled water as the working fluid.

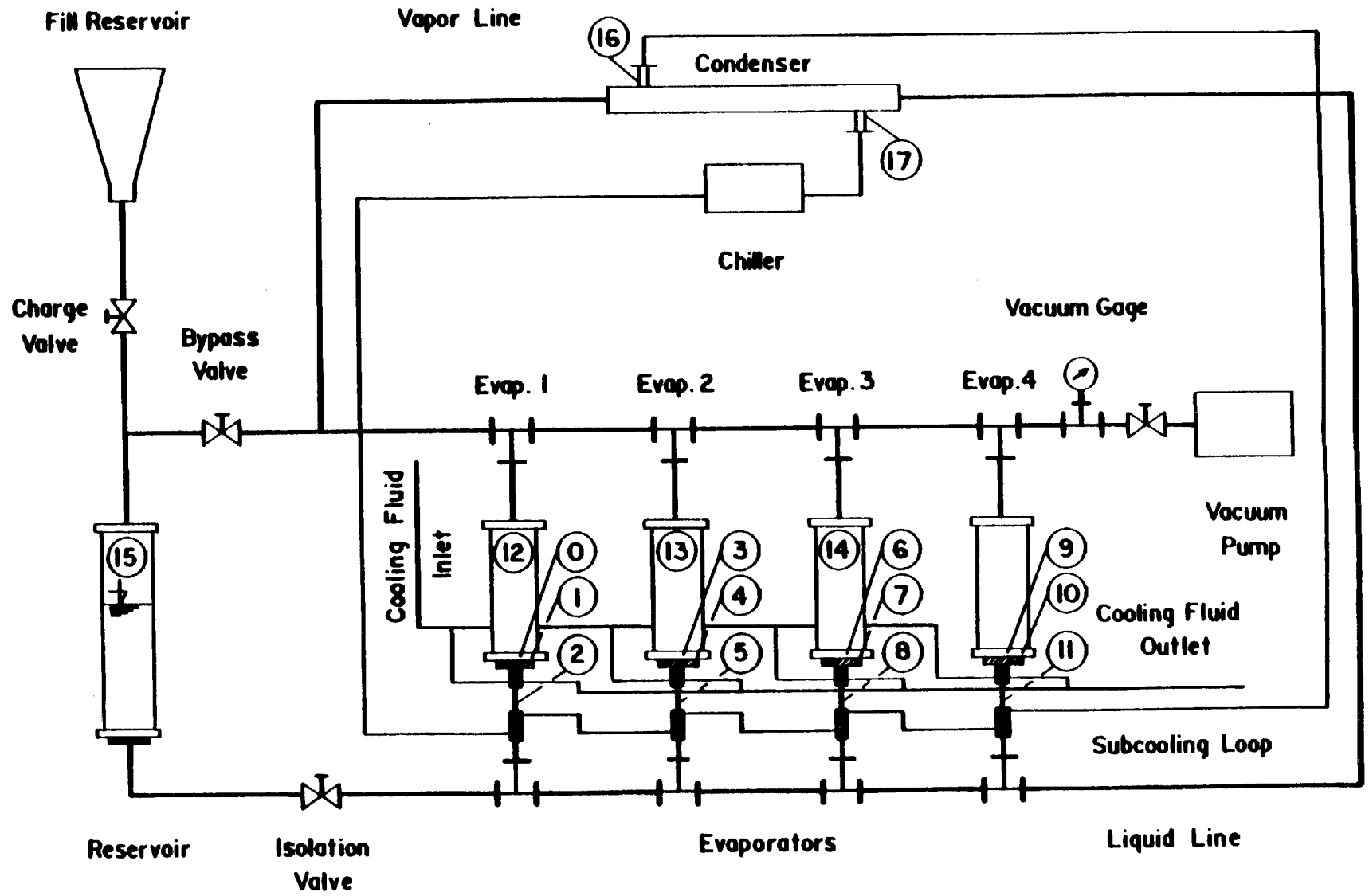

Fig. 2 - Thermocouple Locations On the Tabletop Test System

As shown in Fig. 3, each evaporator chamber incorporates two circular shape brass plates (top and bottom). The brass plates enclose the Pyrex glass tube that is 70 mm O.D. and 10 cm in height. The bottom brass plate is heated by a chromalox disk heater of 350 watts maximum capacity. Therefore, the upper side of the brass plate is the heating surface. The wick structure which is placed on top of this plate consists of two layers of 100 mesh brass screen and of four absorbent paper felt layers placed between them. Felt layers are used to improve the capillary action of the wick structure. The liquid vapor interface is formed in the top screen layer to achieve the capillary pressure rise. By using a special wick design arrangement, the bottom screen layer and four absorbent paper felt layers are extended into the vertical liquid inlet pipe in order to bring the liquid into the top composite wick layers by capillary action. Circular edges of the wick layers were sealed and attached tightly to the heating surface by using liquid solder. This would prevent any direct passage between the vapor space and the liquid layer. The wick layer is retained firmly against the heated surface by using an 8 mesh stainless steel top layer and a retaining spring to provide good contact of the wick structure with the heating surface. The evaporator chambers are designed in such a way that

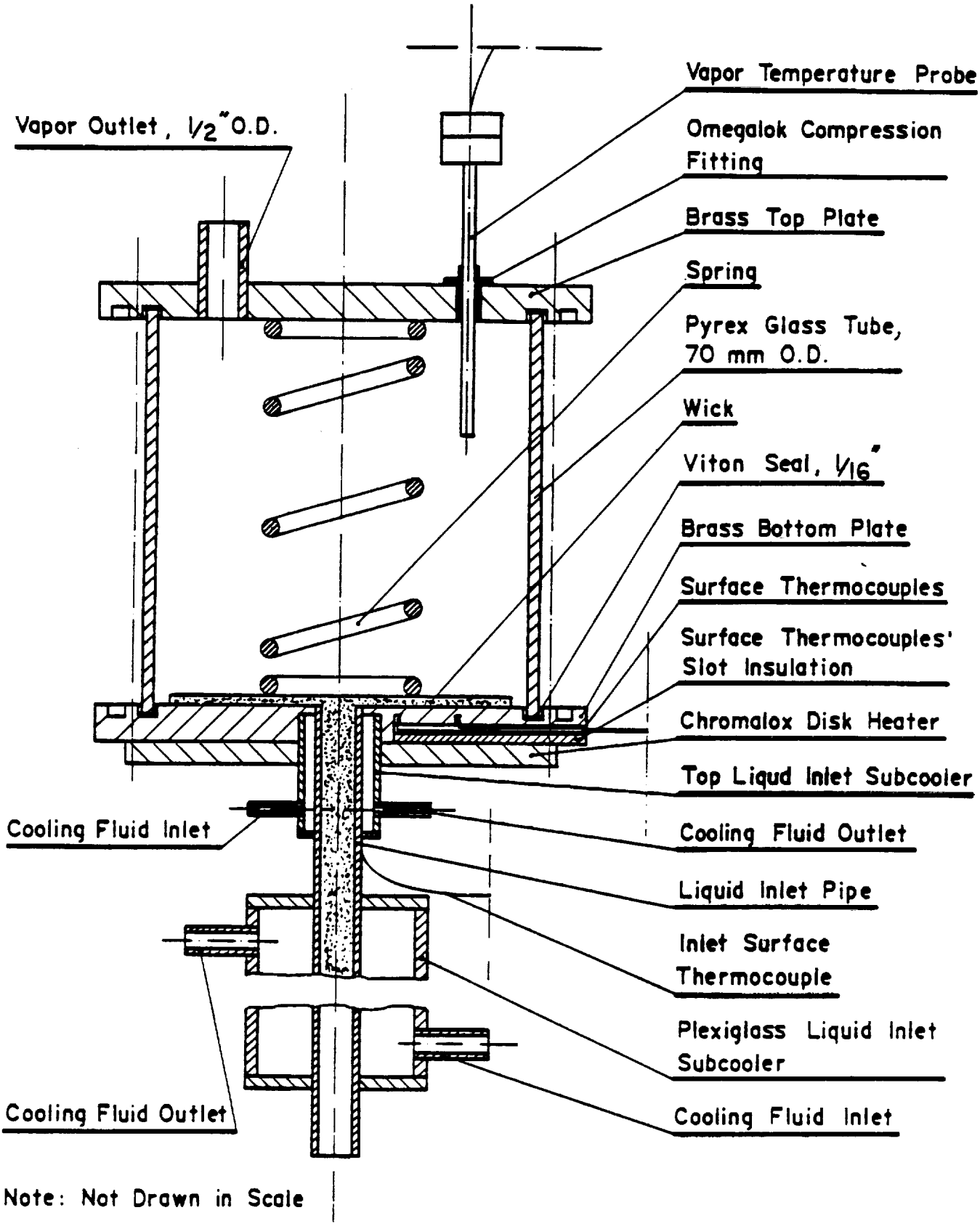

Fig. 3 - Schematic Drawing of the Evaporator Chamber of the Tabletop Test System

the liquid enters two evaporators at the bottom through 1/2 in. O.D. copper tubings and the other two through the same size pyrex glass tubings. Effects of tubing material on the inlet subcooling is discussed in Sec. 5.5.1. A plexiglass liquid inlet subcooler is used to subcool the liquid coming from the liquid line to the evaporator chamber. The coolant to the plexiglass subcooler is supplied by a Neslab Model EX-200 DD Bath Circulator and a Model EN-850 Flow-thru Cooler. Design details and the location of the plexiglass subcooler are shown in Fig.3. During the preliminary test runs, it was observed that the evaporator inlet temperatures were as high as the reservoir temperature, leading to deprime of the test system. It was concluded that with small flow rates of the working fluid, heat gains to inlet pipes from the electric heaters were offsetting the liquid subcooling provided at both the condenser exit as well as the plexiglass subcooler. Therefore, a top liquid inlet subcooler for each evaporator is also installed for additional subcooling. This subcooler is located, as shown in Fig. 3, at the very top of the inlet section. Since the saturation temperature was set at 30 ^{o}C, cold tap water was used as the coolant in the top inlet subcooler.

The condenser consists of a 95 cm long double-pipe heat exchanger made of two concentric 1/2" O.D. and 7/8" O.D. copper tubes. The cooling liquid to the condenser is supplied by the same Neslab Flow-thru Cooler mentioned above.

The test system employs a Model 1399 Welch Duo-Seal Vacuum Pump. Prior to charging with the working fluid, the vacuum pump is used to evacuate the test system and remove the gases released during the out-gassing process. After introducing the working fluid into the test system, the vacuum pump is used again to remove the gases released from the working fluid.

The reservoir is also made of pyrex glass tubing, of 70 mm O.D. and 20 cm in height. It is connected to the loop by a tube exiting at its bottom. It is heated at its bottom by a chromalox disk heater and at the sides by a tape heater of 80 watts maximum capacity to set up and maintain constant reservoir temperature. Operating temperature test of the test CPL System is controlled by adjusting its reservoir temperature. This requires that the reservoir is of sufficient volume to accommodate the range of liquid displacement to maintain variation in the operating conditions. Furthermore, for proper operation, it is also required that the reservoir

contains both liquid and vapor at all times, and that the condenser is always partially blocked.

A fill reservoir of one liter capacity is used to charge the test system with distilled water, the working fluid. This reservoir is connected to the test system by Tygon tubing.

The liquid and vapor lines are made of 1/2" I.D. Tygon brand clear vacuum tubing, 1/2" O.D. copper tubing, and the Swagelok connection fittings. The vacuum type tubing clamps are used to get airtight connections between copper tubing and Tygon tubing.

The evaporator chambers, vapor line, condenser, and reservoir are insulated in order to reduce the heat losses from the test system to the environment. As shown in Fig. 2, the test system is instrumented with 18 thermocouples. These thermocouples provide temperature readings around the loop which are monitored using the data acquisition and control system of the test loop. Temperature readings are displayed in real time on the IBM PC screen. Description of temperature and power channels employed by the data acquisition and control system are shown in Table 1 and Table 2.

Table 1 - Description of Temperature Channels Employed by the Data Acquisition and Control System of the Tabletop Test System

CHANNEL #	
0	Center Surface Temperature of Evaporator 1
1	Middle Surface Temperature of Evaporator 1
2	Inlet Pipe Temperature of Evaporator 1
3	Center Surface Temperature of Evaporator 2
4	Middle Surface Temperature of Evaporator 2
5	Inlet Pipe Temperature of Evaporator 2
6	Center Surface Temperature of Evaporator 3
7	Middle Surface Temperature of Evaporator 3
8	Inlet pipe Temperature of Evaporator 3
9	Center Surface Temperature of Evaporator 4
10	Middle Surface Temperature of Evaporator 4
11	Inlet Pipe Temperature of Evaporator 4
12	Vapor Temperature of Evaporator 1
13	Vapor Temperature of Evaporator 2
14	Vapor Temperature of Evaporator 3
15	Reservoir Temperature
16	Condenser Inlet Temperature of Cooling Fluid
17	Condenser Outlet Temperature of Cooling Fluid

Table 2 - Description of Power Channels Employed by the Data Acquisition and Control System of the Tabletop Test System

CHANNEL #	
32	Power Input to Evaporator 1
33	Power Input to Evaporator 2
34	Power Input to Evaporator 3
35	Power Input to Evaporator 4
36	Power Input to Reservoir

5.2 Data Acquisition and Control System

In general, any kind of research work, including experimental testing of a test rig, needs an appropriate data acquisition and control system to support it. Therefore, the data acquisition and control system can provide a better insight in the performance of the experimental test rig under consideration.

Each data acquisition and control system consists of hardware and software. The hardware consists of the following basic elements: DAS-8 (MetraByte) A/D board, SRA-01 relay board, IBM XT PC, Tektronix 4662 plotter, and three variacs with their corresponding switchboard. The most important element of the hardware is DAS-8 A/D board which, more or less, determines the basic characteristics and limits of the data acquisition and control system. The Board is an 8 channel, 12 bits high speed A/D converter for the IBM PC. The full scale input of each channel is +/-5 volts with a resolution of 0.002434 volts, 2.44 millivolts. This means that -5 volts is equivalent to 0 bits, and +5 volts is equivalent to 4096 bits. A/D conversion time is typically 25 microseconds, 35 microseconds maximum. The expansion multiplexer,

multiplexes 16 differential inputs to a single analog output suitable for connection to any of the analog input channels of DAS-8. The MetraByte board used in the Heat Transfer Laboratory has three multiplexer boards or 48 available channels. A cold junction correction sensor is also included for software compensation of thermocouples which can be directly connected to the multiplexer. DAS-8 requires 8 consecutive address locations in I/O space. The data is combined in the following way:

$$V = ((X*10)/4096 - 5)/G$$

where,

V - data in volts

X - data in bits

10 - span (-5 volts; + 5 volts)

5 - substraction zero offset, - 5 volts

G - Gain

SRA-01 relay board is used to allow the control of the power input to the reservoir. Namely, when the reservoir temperature is above the reference value, the power is turned off. On the other hand, when the reservoir temperature is below the reference value, the power is turned on.

Three variacs are used for the control of power inputs to the test system, i.e., one variac for the power input to the reservoir, while two other variacs for the power inputs to the evaporators. These variacs are accompanied by the switchboard which includes three ammeters and voltmeters.

The software of the data acquisition and control system was written in Turbo Pascal 4.0. It consists of two groups of programs. The first group deals primarily with real time programming. Considering the present test system, the first group of programs gives, in real time, data values of the chosen channels in terms of the numerical values, and curves on the IBM PC screen. Furthermore, this first group generates data files in which it stores the data of the test runs. The second group of programs retrieves the stored data from already generated files by the first group and plots the selected data channels on different output devices, such as IBM PC screen, Tektronix plotter and IBM plotter. This group covers all the data channels of the test system used by the data acquisition and control system. Every 2 seconds it gives the numerical values of the data channels, while every 48 seconds plots ten selected data channels on the IBM PC screen. Throughout the test runs the

programs of this type generate the data files, if it is requested.

The developed data acquisition and control system provides enormous flexibility in collecting and evaluating the data of the Tabletop Test System.

The test loop is instrumented as shown in Fig. 2. Sensor outputs are connected to the data acquisition system for data collection and display.

5.3 Preparation of the Test Loop

Prior to incorporation in the loop, all of the components used in the test loop were cleaned either by distilled water or acetone. To test cleanliness of the capillary wicks, drops of distilled water were added to the cleaned surfaces. Immediate spreads across the surfaces indicated that good wetting characteristics and, therefore, satisfactory cleanliness had been achieved.

Following cleaning, the test rig was assembled and purged with dry nitrogen to remove the moisture from the loop. Then the loop was closed and vacuumed while all the heaters were on. Next, the loop was leak tested, and the several leaks detected at the loop connectors were

fixed. Afterwards, the test loop was charged with approximately 700 cc distilled water. This fluid charge was sufficient to fill the sum of volumes of the condenser, liquid line, and the evaporators to the wick level. In order to guarantee start-up under the minimum power input conditions, an additional 20% is added to the calculated volume.

5.4 Start-up Procedure of the Test System

The preliminary testing of the CPL System led to adoption of the following start-up procedure:

- Start the data acquisition and control system and check that all sensors read nominal values.

- Check the vacuum gage and make sure that there is no decrease in the vacuum pressure. If there is any decrease in the vacuum pressure, locate leaks by pressurizing the system with dry nitrogen and remove noticed leaks.

- Evacuate the test system once more.

- Start-up the chiller, and set the heat sink temperature at 0 C. Furthermore, start running the

tap water through the top liquid inlet subcoolers at a mass flow rate of 0.7 (lit/min) per subcooler.

- Set the reservoir temperature controller to 30 ^{o}C and set the power to 50 watts. At the same time, set the evaporator power to 50 watts per evaporator while the total system is at 200 watts.

- After 15 minutes, increase the evaporator power to 125 watts per evaporator while the total system power is 500 watts.

- If, after 15 minutes no evaporator has deprimed, the start-up was successful.

Initial testing established that power levels less than 50 watts per evaporator could not be supported without causing deprime of any evaporators during the start-up. However, it should be mentioned that it was not possible to eliminate completely the heat loss from the electric heaters. As a result, the actual start-up power input to each evaporator was expected to be significantly less than 50 watts.

Figures 4 and 5 show the temperature responses of Evaporator 1 and Evaporator 2 during successful start-ups. Furthermore, these figures also exhibits the steady state performance of these evaporators at 125 watts per evaporator power input level. Similar performances were also obtained for Evaporator 3 and Evaporator 4.

5.5 Test Results

Transient behavior of the bench-top CPL test system was evaluated experimentally during operation by applying a sequence of step heat pulses to the evaporators. System characteristics were obtained by recording time variation of the evaporator heating surface temperature above the saturation temperature. Furthermore, the test data was collected to provide the heat transport limit of the CPL System under given operation modes. The heat transport limit is reached when the pressure drop sustained by any evaporator in the Capillary Pumped Loop becomes equal to the capillary pressure that can be developed by the wick in that evaporator. The transport limit is dependent on many parameters, so it varies with different operating conditions.

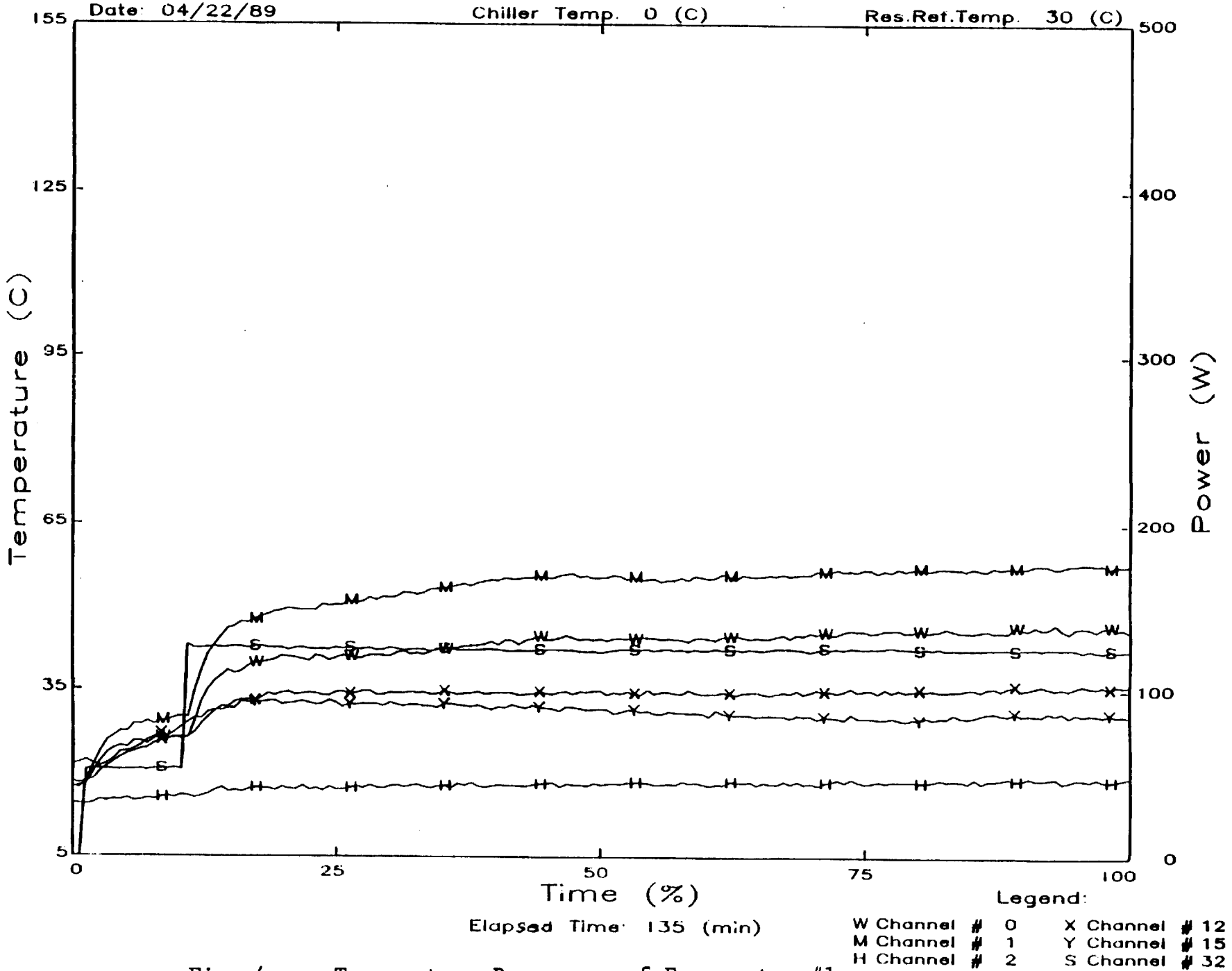

Fig. 4 - Temperature Responses of Evaporator #1 During and After Successful Startup

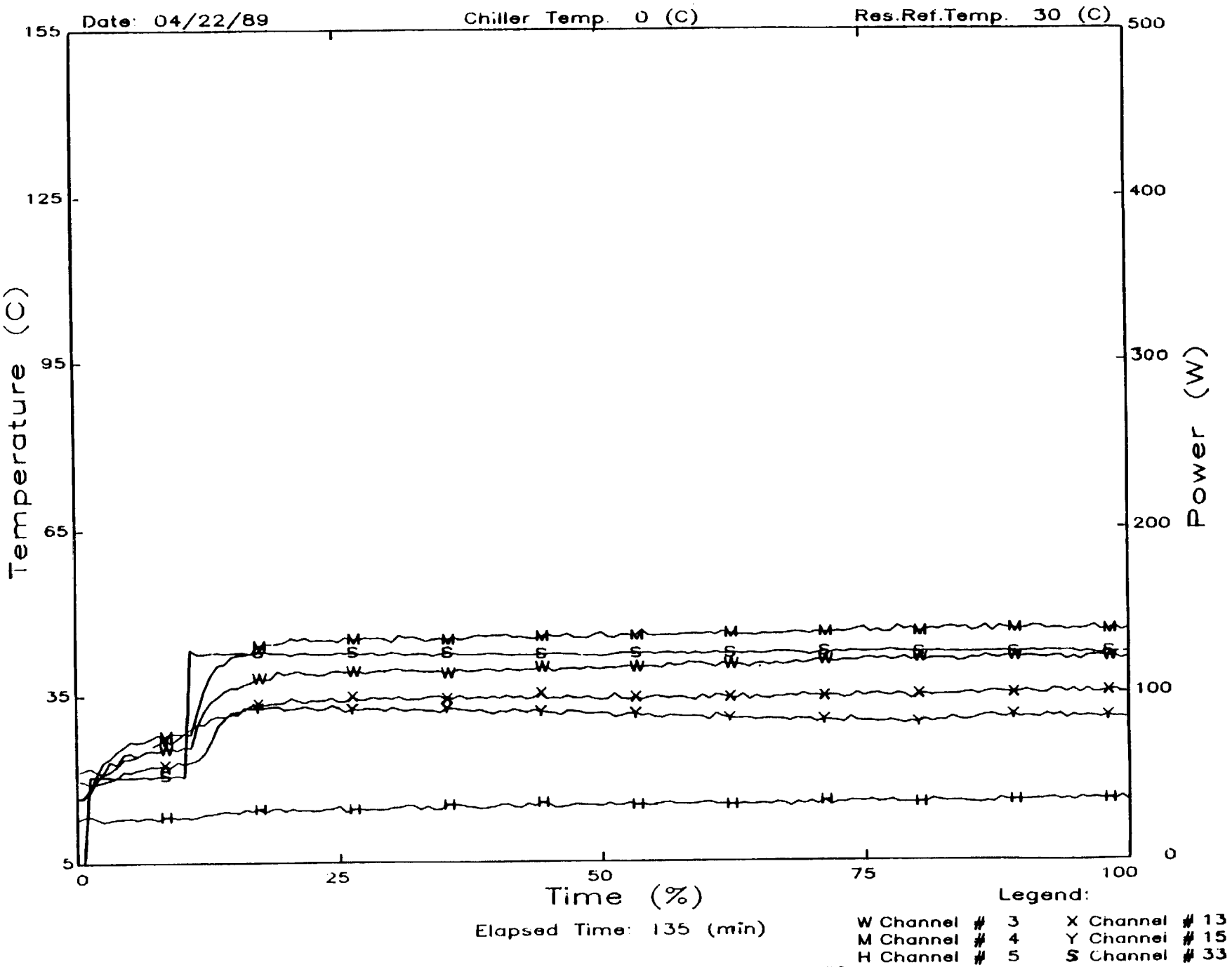

Fig. 5 - Temperature Responses of Evaporator #2 During and After Successful Startup

Initially, effects of the inlet sub-cooling and the sink temperature on transient performance of the test system were studied. Due to design limitation of the test setup, the elevation of the wick level with respect to that of the condenser was not changed in the test runs. Furthermore, the reservoir reference temperature could not be changed significantly since it would have required adoption of a new start-up procedure. The reservoir reference temperature was kept at 30 ^{o}C. the average elevation between the wick and the condenser was 2 cm.

In the initial test runs, it was expected that after a successful start-up the power input could be increased to all four evaporators in a step-wise manner until the heat transport limit is reached. This limit would be characterized by a continuous rise of the evaporator surface temperature without approaching a steady state. However, it was observed that any simultaneous increases in the evaporator power inputs, following a successful start-up, would leave the condenser without any liquid phase and flush the reservoir with liquid. These results indicated that size of the condenser was not large enough to condense the water vapor at higher power inputs in such a way that the condenser would be partially blocked at all times. Without partial blockage conditions, vapor

would completely fill the condenser and flush the reservoir with liquid. Under such conditions, proper operation of the test system could not be maintained. Proper operation requires that the operating temperature of the Capillary Pumped Loop is controlled by temperature of the reservoir, provided that the reservoir contains both liquid and vapor phases of the working fluid under all conditions, and a partially blocked condenser is maintained at all times.

After further testing, it was determined that by increasing the power input to only one evaporator at a time, and keeping others at low power inputs (50 watts per evaporator), it was possible to maintain the proper operating conditions. Since the main purpose of the present experiments was to study the transient CPL performance rather than to determine the overall heat transport capability of the test system, following a start-up, power was increased step-wise only to one evaporator while the others were each kept at 50 watts. Every 20 minutes, the power input was increased by 50 watts to the same evaporator until the transport limit had been reached.

5.5.1 Evaporator Inlet Sub-cooling

Preliminary performance test runs showed that the evaporators employing copper inlet tubing could withstand power inpute of 350 watts, which is the maximum capacity of the electric heater. Considering the evaporators with the pyrex glass inlet tubings, even when the recorded outside surface temperatures of the glass tubings were below the reservoir temperature, these evaporators deprimed as soon as the power inputs to each evaporator was increased to 50 watts. This is attributed to low conductivity of the pyrex glass compared to that of copper. Since, thermal resistance of the pyrex tube to the coolant was very large, inlet liquid temperature remained greater than the reservoir temperature despite the fact that the outside pyrex tube temperature was lower than this temperature. Therefore, the pyrex glass inlet tubes were replaced by copper tubings.

5.5.2 Transient Performance of the Test System

Transient temperature responses of evaporators 1 and 2 were investigated by applying step power inputs to one of these evaporators at a time while keeping the power inputs to other evaporators at 50 w each.

Transient responses were investigated at two different sub-cooling fluid flow rates of 0.1 and 0.7 lit/min. By using an adjustable clamp, the coolant flow rate was controlled to the evaporator under consideration, while the other evaporators were having the fixed mass flow rate of 0.7 lit/min each.

Transient temperature test data is shown in Figs. 6 to 9. In these figures, time variations of both the center and the middle evaporator heating surface temperatures were shown when the power inputs was increased in 50 w steps. Between each step, the test system was allowed sufficient time to reach a steady state; until the transport limit was obtained. This limit characterized by a continuous rise of the heating surface temperature without approaching steady state. On the basis of this test data, it is noted that

- With 0.1 lit/min sub-cooling flow rate, evaporator dryout occurred when power input was increased to 150 w. Whereas, with 0.7 lit/min flow rate, the test system operated properly without dryout up to the maximum power input of the electric heater, 350 w.

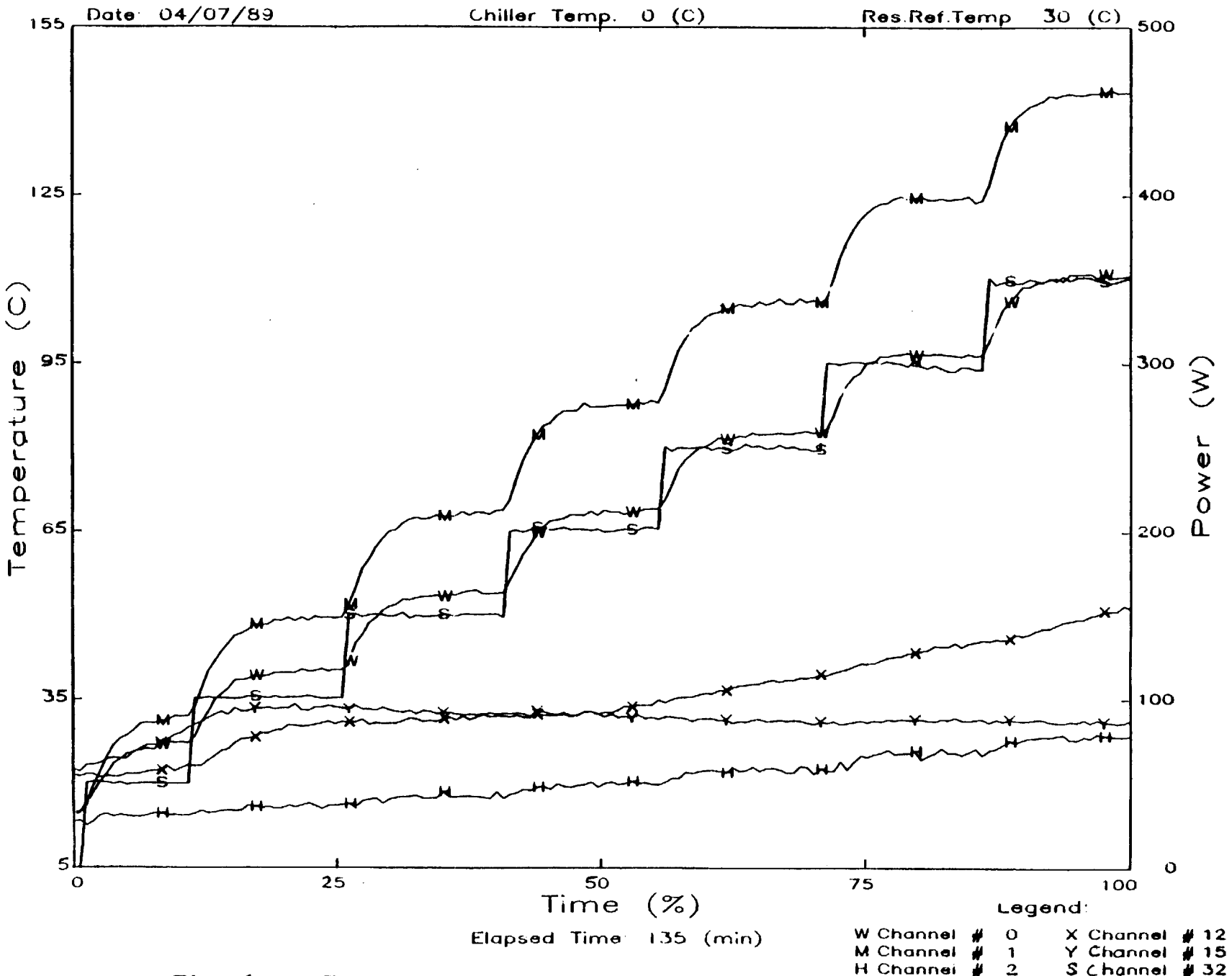

Fig. 6 - Temperature Responses of Evaporator #1 During Test Run at Mass Flow Rate of 0.7 (l/min)

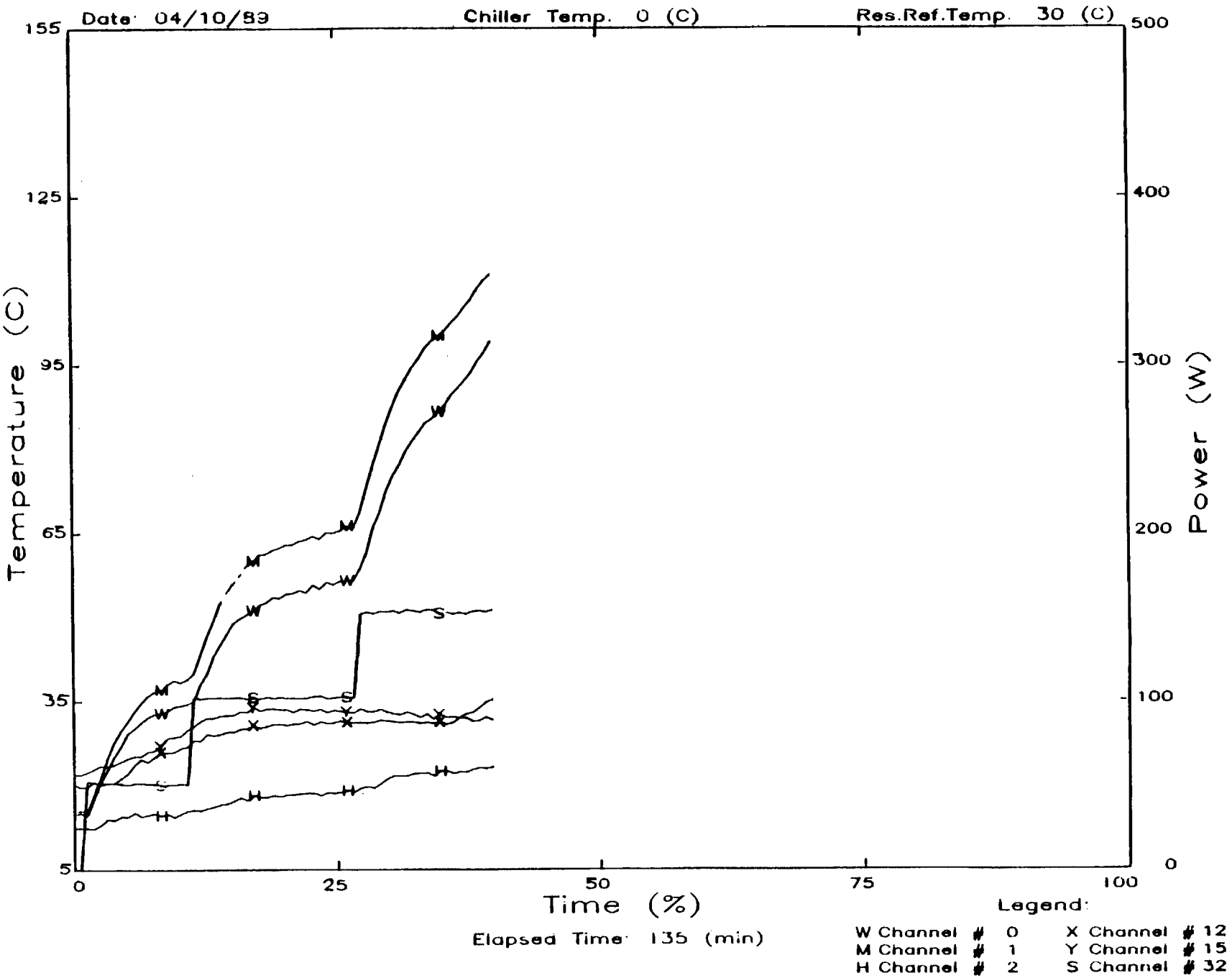

Fig. 7 - Temperature Responses of Evaporator #1
During Test Run at Mass Flow Rate of 0.1 (l/min)

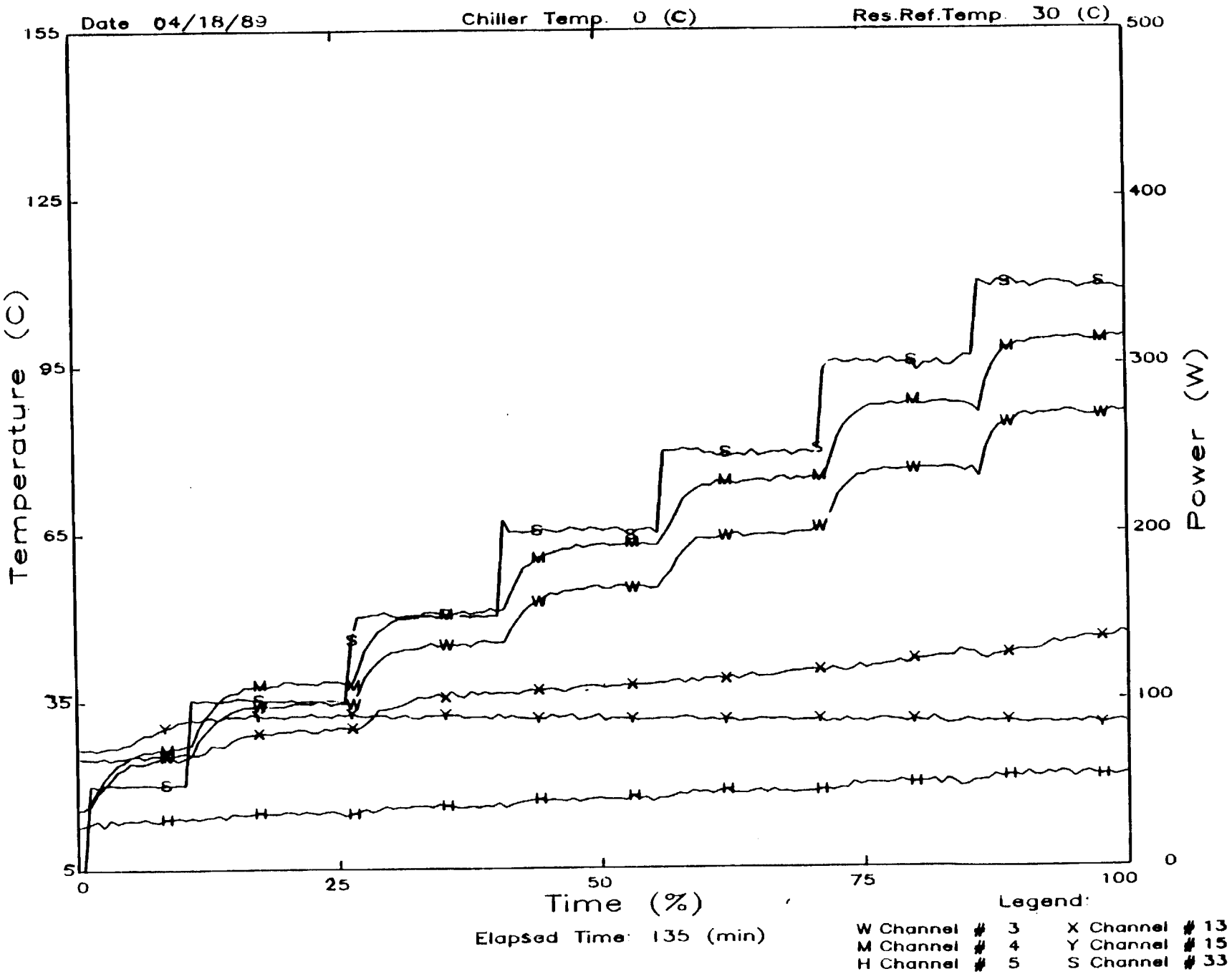

Fig. 8 - Temperature Responses of Evaporator #2 During Test Run at Mass Flow Rate of 0.7 (l/min)

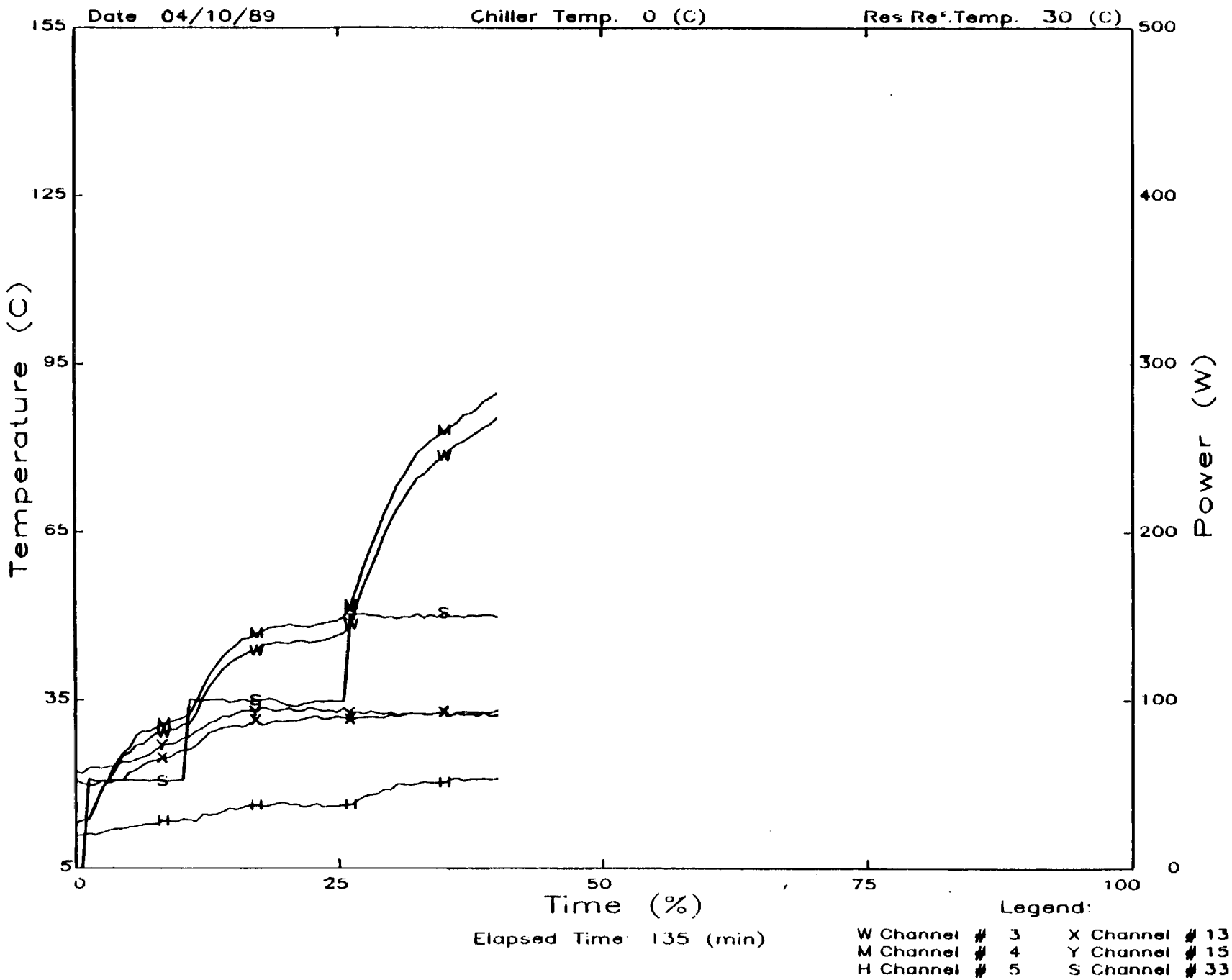

Fig. 9 - Temperature Responses of Evaporator #2
During Test Run at Mass Flow Rate of 0.1 (l/min)

- Evaporator surface temperatures measured at two locations were changed step-wise in an expected fashion without any unusual behavior; such as exhibiting any oscillatory tendencies. Surface temperature closer to the liquid inlet remained lower than that at the location farther from the inlet. This indicated that the heating surface was not isothermal.

- Although the reservoir temperature remained constant, vapor temperature increased somewhat with increased power input. This was attributed to vapor superheating caused by non-isothermal temperature condition along the evaporator heating surface. Inlet pipe temperature also was increased slightly with increasing power input.

- It is noted that with proper inlet sub-cooling, evaporator surface temperature reached steady state values following each step increase in the power input to the evaporator.

Tests were repeated at 0.2, 0.3, 0.5, and 0.6 lit/min subcooling flow rates. Except with the flow rate of 0.2 lit/min, the characteristic transient

temperature changes were observed without any dryout, up to the maximum power input of 350 w. With 0.2 lit/min subcooling flow rate, the heat transport limit was reached for both evaporators 1 and 2.

5.5.3 Heat Transport Limit

Thermal performance of an evaporator in a CPL system can be described by a graph which gives ΔT in terms of power input. Here, ΔT is the difference between the evaporator surface temperature and the working fluid saturation temperature. As the power input to the evaporator increased beyond the transport limit, ΔT would keep rising without bound, unless the power was reduced. This would represent the dryout conditions.

As mentioned earlier, design characteristics of the test system did not allow simultaneous heat loading of all four evaporators. Therefore, it was not possible to determine heat transport limit of the entire test system. Performance was tested by increasing step-wise the power input to only one evaporator while keeping other evaporators at the same low power inputs.

All ΔT versus power input plots given in the present experimental work are based on the linear regression and the values were taken after a period of 20 minutes following a step increase in the power input. Figures 10 through 16 present the thermal performance plots for middle and center surface temperatures Evaporator 1 and Evaporator 2 for different inlet subcooling fluid flow rates varying from 0.1 to 0.7 lit/min. In all these test runs, the reservoir temperature set point was 30 ^{o}C.

Test data in these figures clearly indicate effect of the evaporator inlet subcooling on the test system performance. At a given power, evaporator surface temperture decreases with increased inlet subcooling. As expected, the heat transport limit is delayed with increased subcooling liquid flow rate, i.e., increased inlet subcooling. Again, as noted before, due to limited maximum electric heater capacity, 350 w, the heat transport limit could not be reached with subcooling flow rates greater than 0.2 lit/min.

At a given power input, differences between the middle and the center evaporator surface termperatures, Figs. 11, 12, 15 and 16, show that the working fluid is not distributed evenly in the wick structures; outer

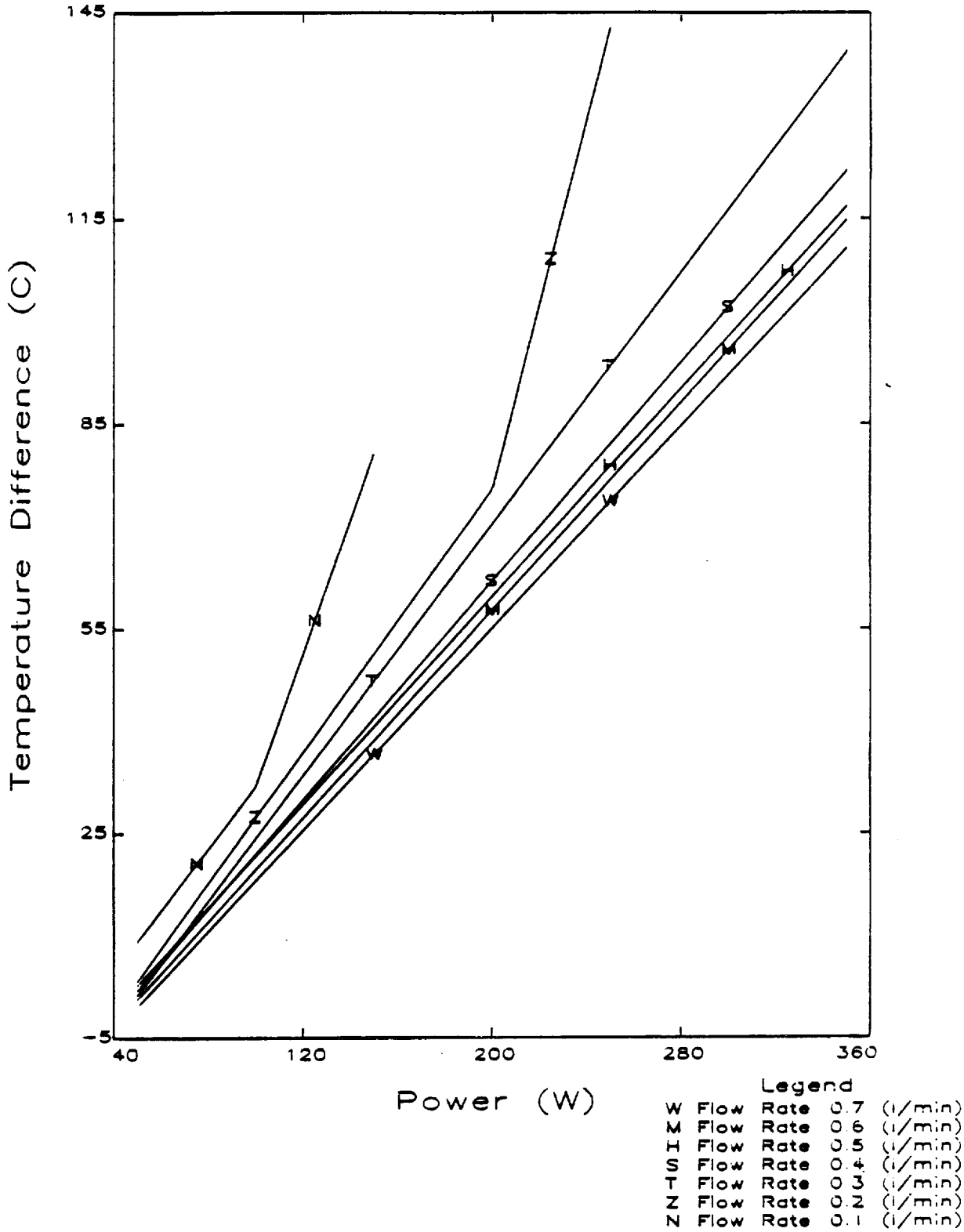

Fig. 10 - ΔT vs. Power Plot for Middle Surface Temperature of Evaporator #1 Different Mass Flow Rates

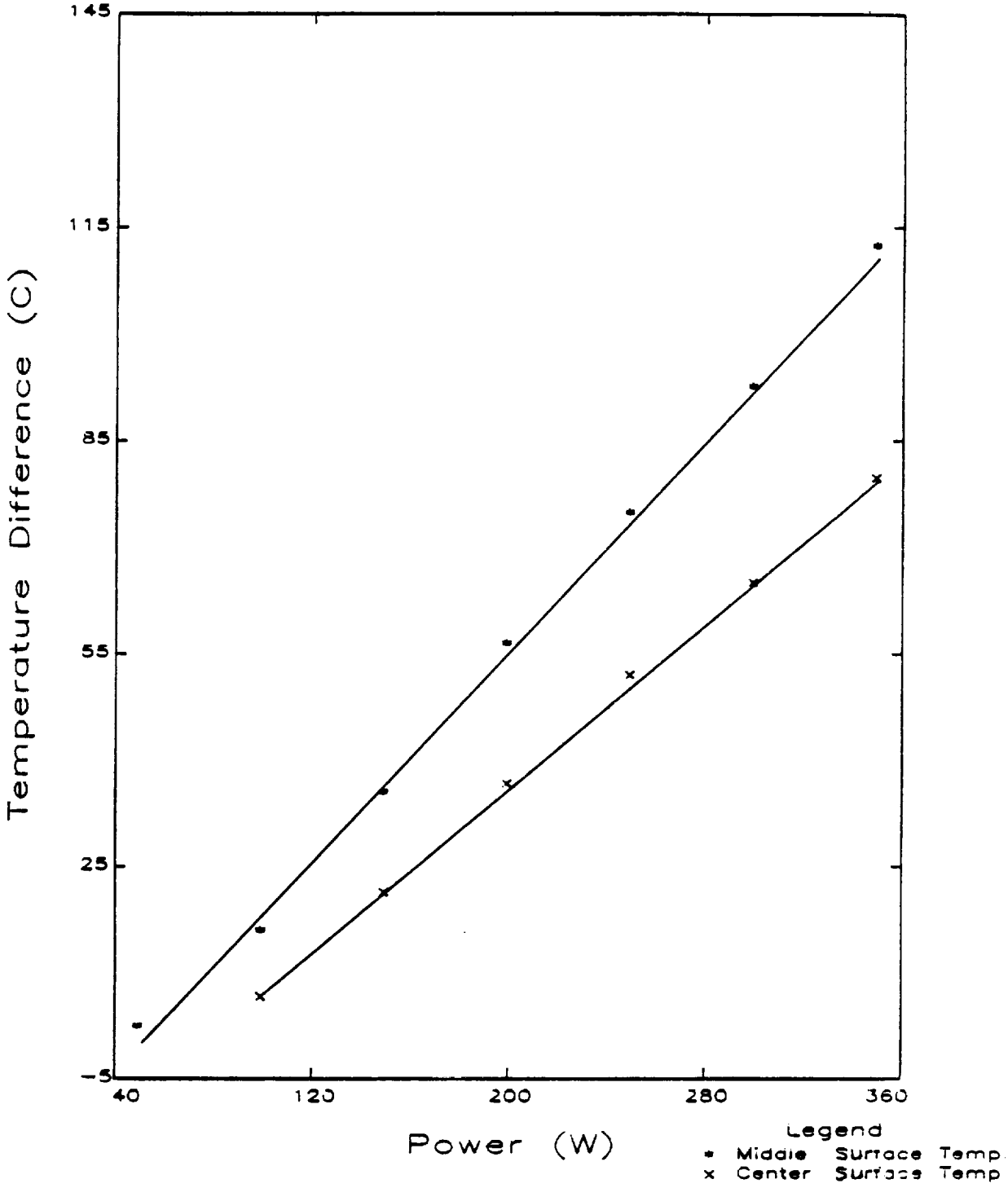

Fig. 11 - ΔT vs. Power Plot for Middle and Center Surface Temperatures of Evaporator #1 During Test Run at Mass Flow Rate of 0.7 (l/min)

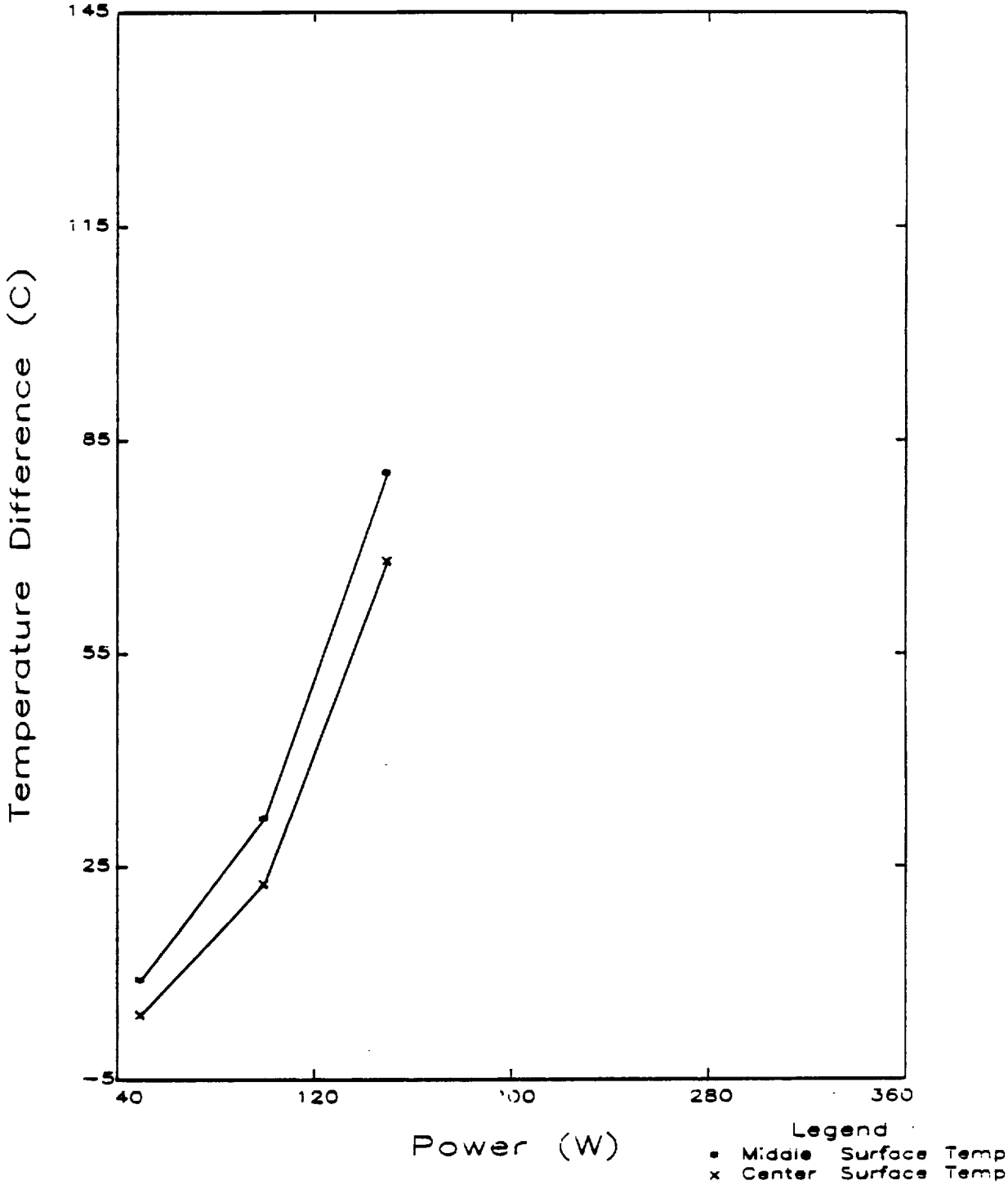

Fig. 12 - ΔT vs. Power Plot for Middle and Center Surface Temperatures of Evaporator #1 During Test Run at Mass Flow Rate of 0.1 (l/min)

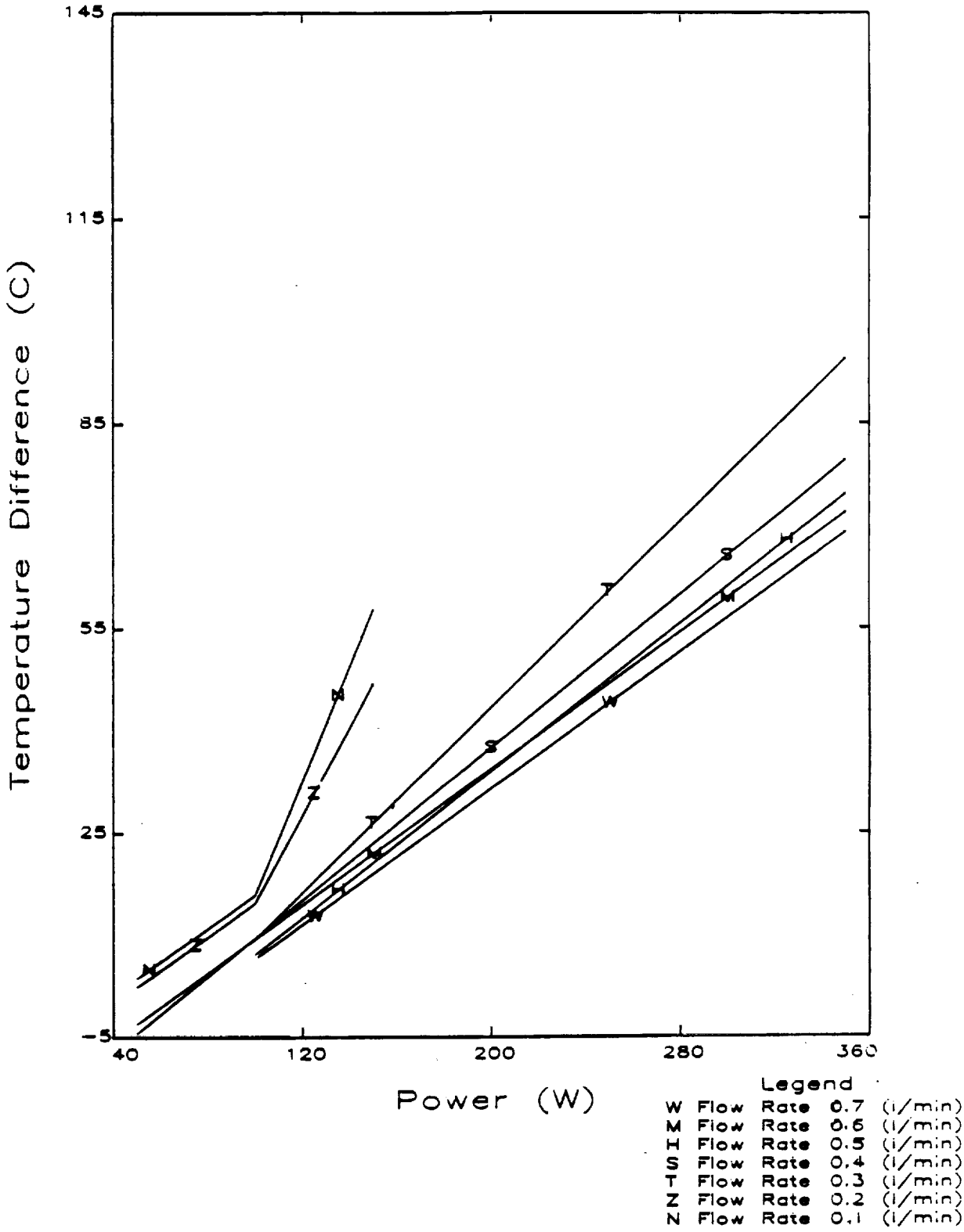

Fig. 13 - ΔT vs. Power Plot for Middle Surface Temperature of Evaporator #1 for Different Mass Flow Rates

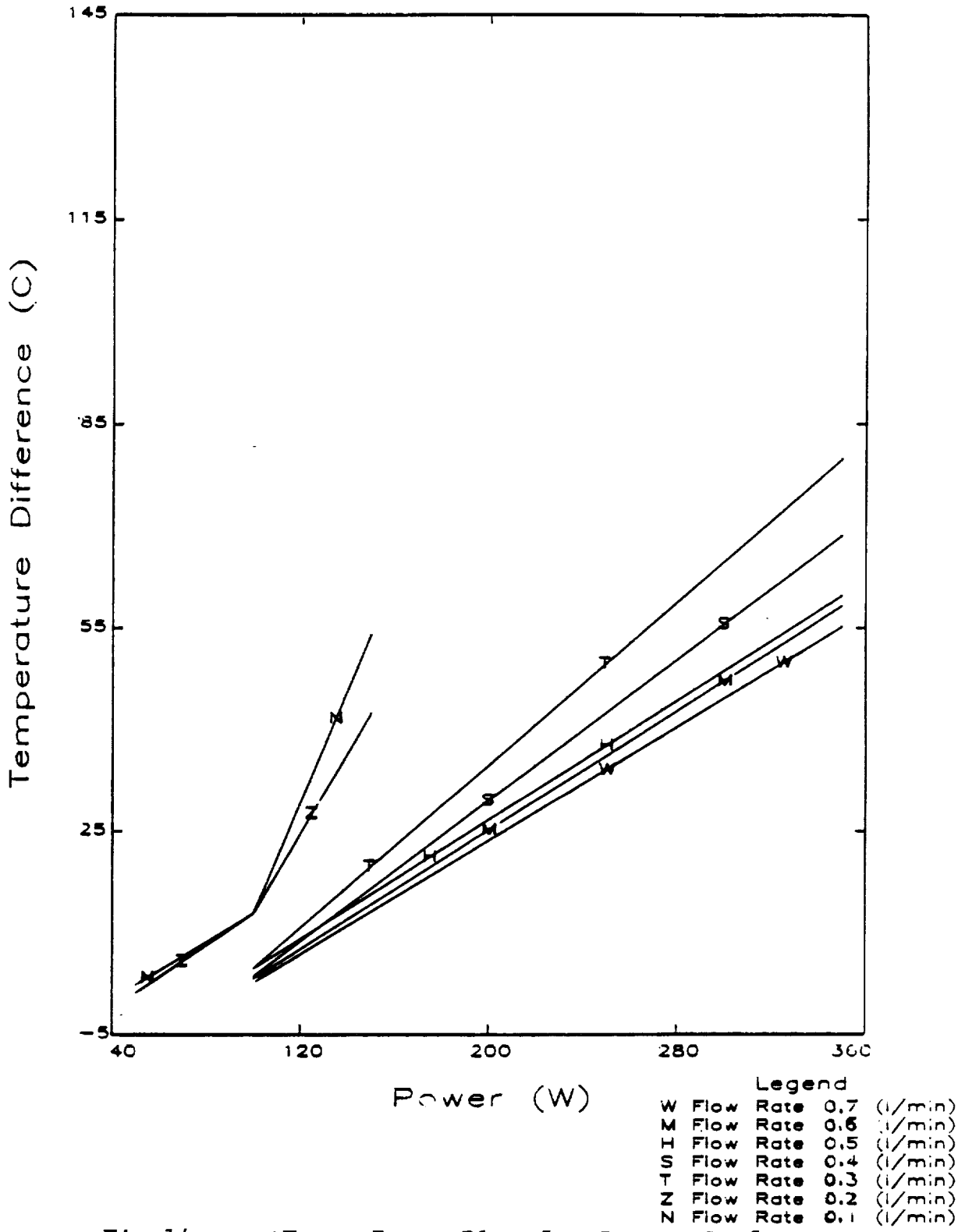

Fig 14 - ΔT vs. Power Plot for Center Surface Temperature of Evaporator #2 for Different Mass Flow Rates

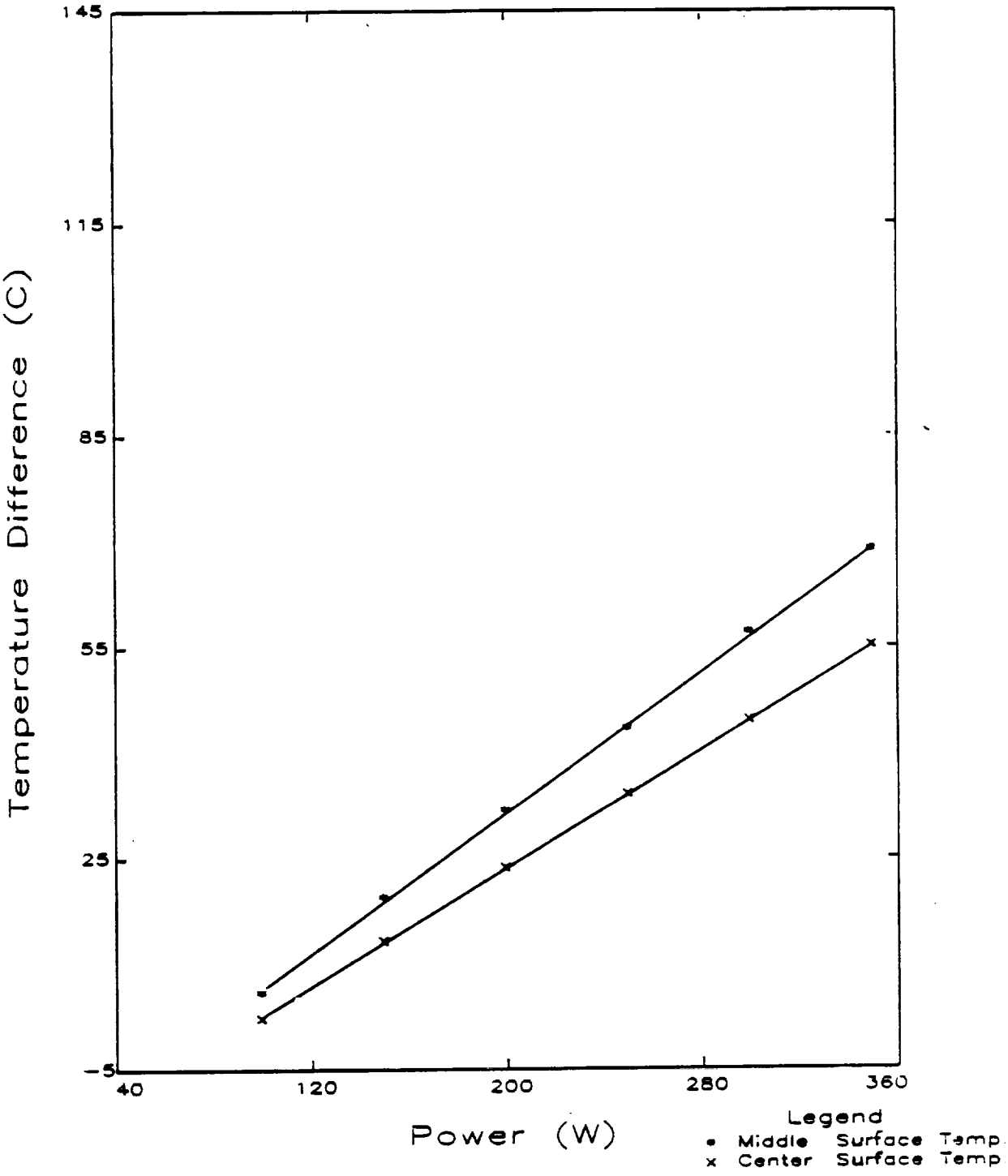

Fig. 15 - ΔT vs. Power Plot for Middle and Center Surface Temperatures of Evaporator #2 During Test Run at Mass Flow Rate of 0.7 (l/min)

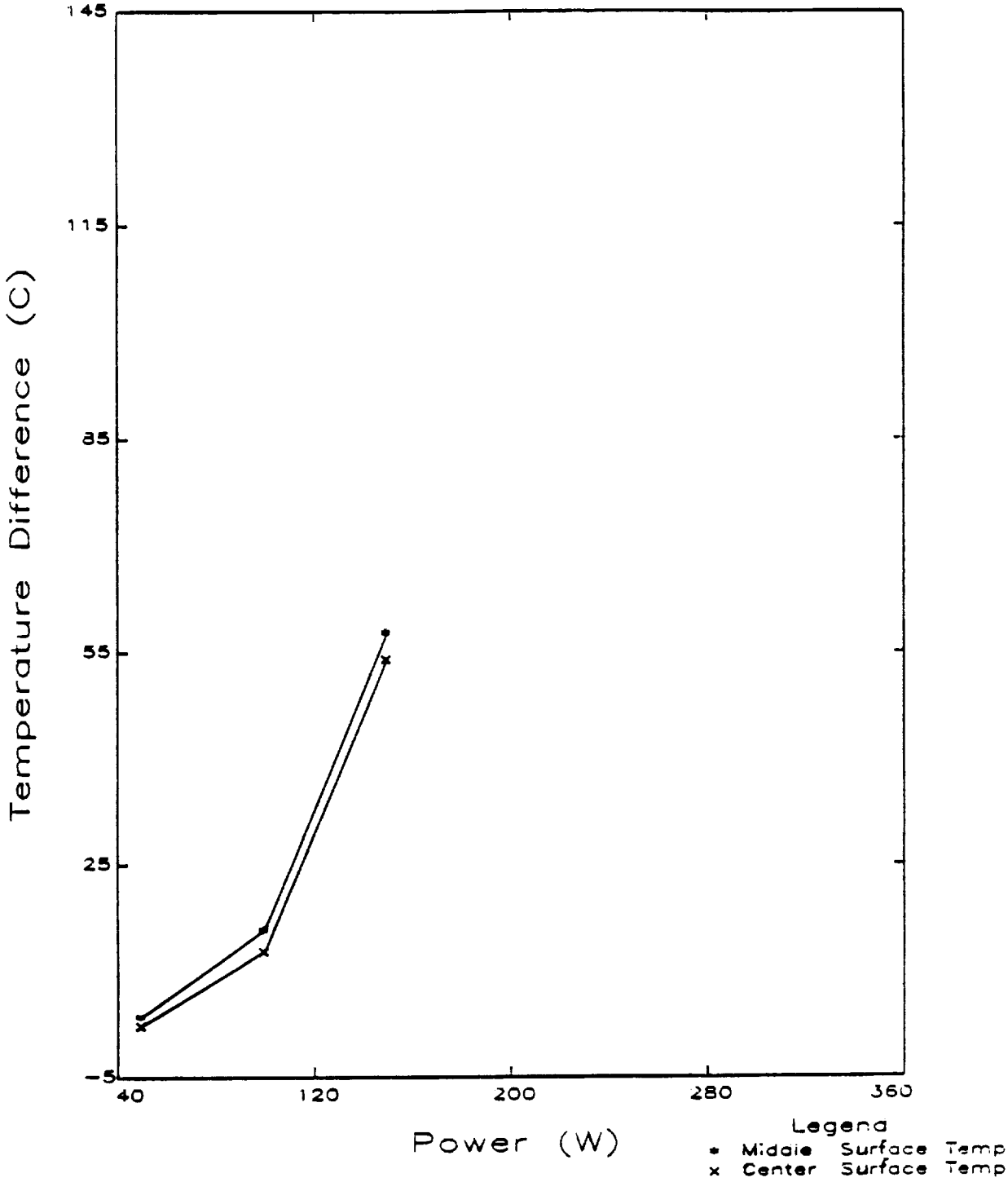

Fig. 16 - ΔT vs. Power Plot for Middle and Center Surface Temperatures of Evaporator #2 During Test Run at Mass Flow Rate of 0.1 (1/min)

regions receiving less liquid. This develops an increasing temperature gradient in the radial direction. The mentioned temperature difference becomes larger at higher power inputs. The recorded temperature gradient conditions help to explain evaporator vapor superheating shown in Figs. 6 to 9. Visual observations of the wick structure indicated that the dryout started from edge of the wick and moved gradually toward the evaporator liquid inlet. The partial wick dryout, however, did not interrupt the evaporator operation, although caused some vapor superheat.

The test system could operate properly as long as there was enough subcooling at the inlet of the evaporator. It is expected that when the inlet temperature increases above the saturation, the evaporator would deprime. Referring to temperature variations in Figs. 7 and 9, however, it is noted that evaporators 1 and 2 deprimed despite the fact that the inlet pipe temperatures seemingly remained below the saturation temperature. This anomaly can be explained by referring, in Fig. 2, to locations of inlet pipe temperature sensors. Since these sensors were placed at upstream side of the top subcoolers and, since these coolers were in close proximity of the electric heaters, the actual liquid temperature entering the evaporators

were greater than that measured by the temperature sensors.

In subsequent tests, effect of the heat sink temperature on performance was studied for Evaporator 2. The mass flow rate of the inlet subcooling was kept constant at the rate of 0.7 (1/min), while the chiller temperature was varied and had the following values: -5, 0, and 5 degree C. Figures 17 and 18 present the thermal performance plots for the middle and the center surface temperature variations of Evaporator 2 for different chiller temperatures. At a given power input, ΔT values increased with increasing chiller temperature. Furthermore, it is seen that in the region closer to the liquid inlet to the evaporator, effect of change in the heat sink temperature is more significant.

6. TRANSIENT ANALYSIS OF CPL HEAT PIPE

In transient operation of the CPL System, temperatures of various components do not change uniformly. Therefore, the isothermal heat pipe models used in earlier studies cannot be utilized for predicting the transient thermal CPL performance. In the present analytical investigation, a lumped-heat capacity model of the CPL heat pipe has been developed by assuming that

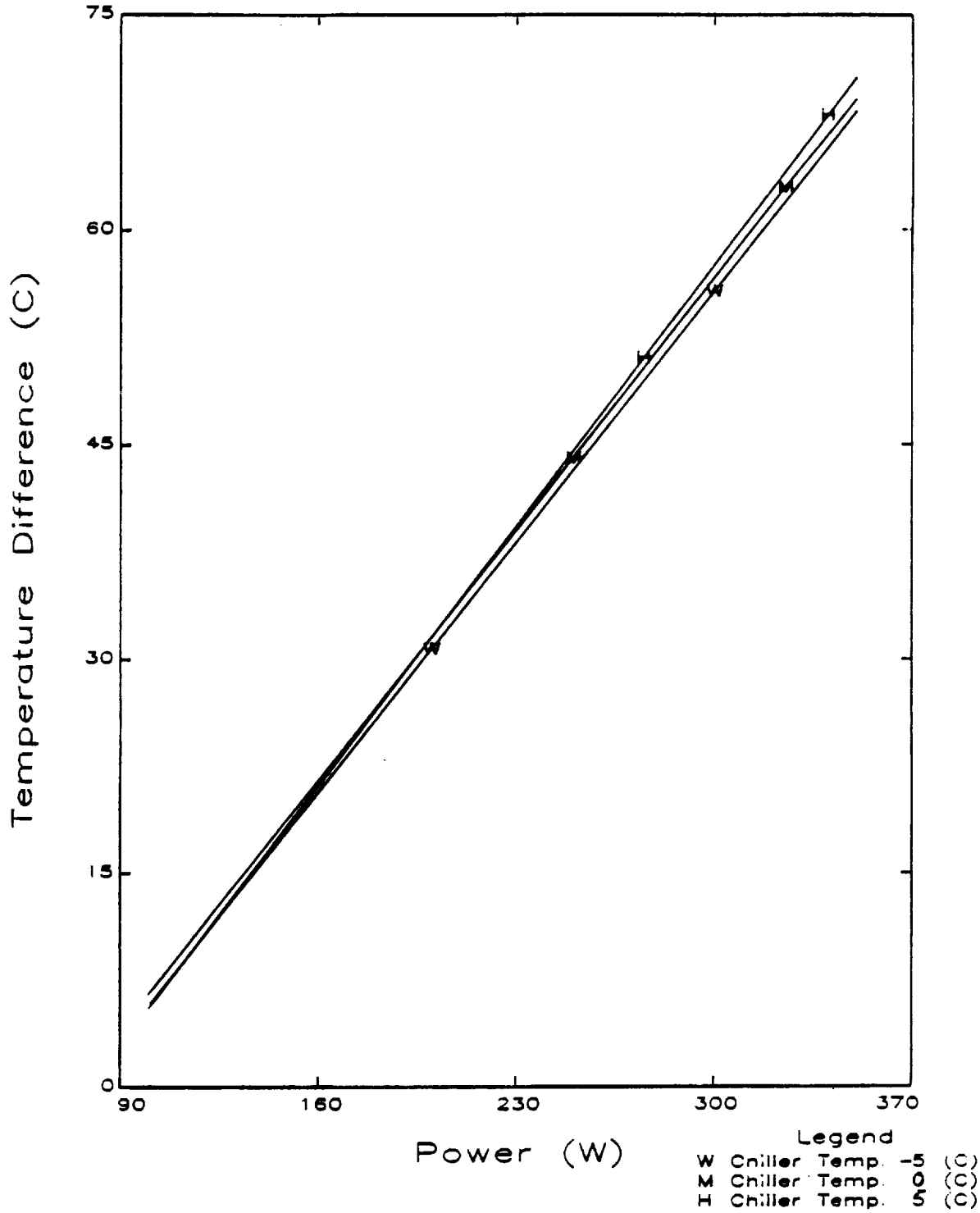

Fig. 17 - ΔT vs. Power Plot for Middle Surface Temperature of Evaporator #2 for Different Chiller Temperatures and at Mass Flow Rate of 0.7 (l/min)

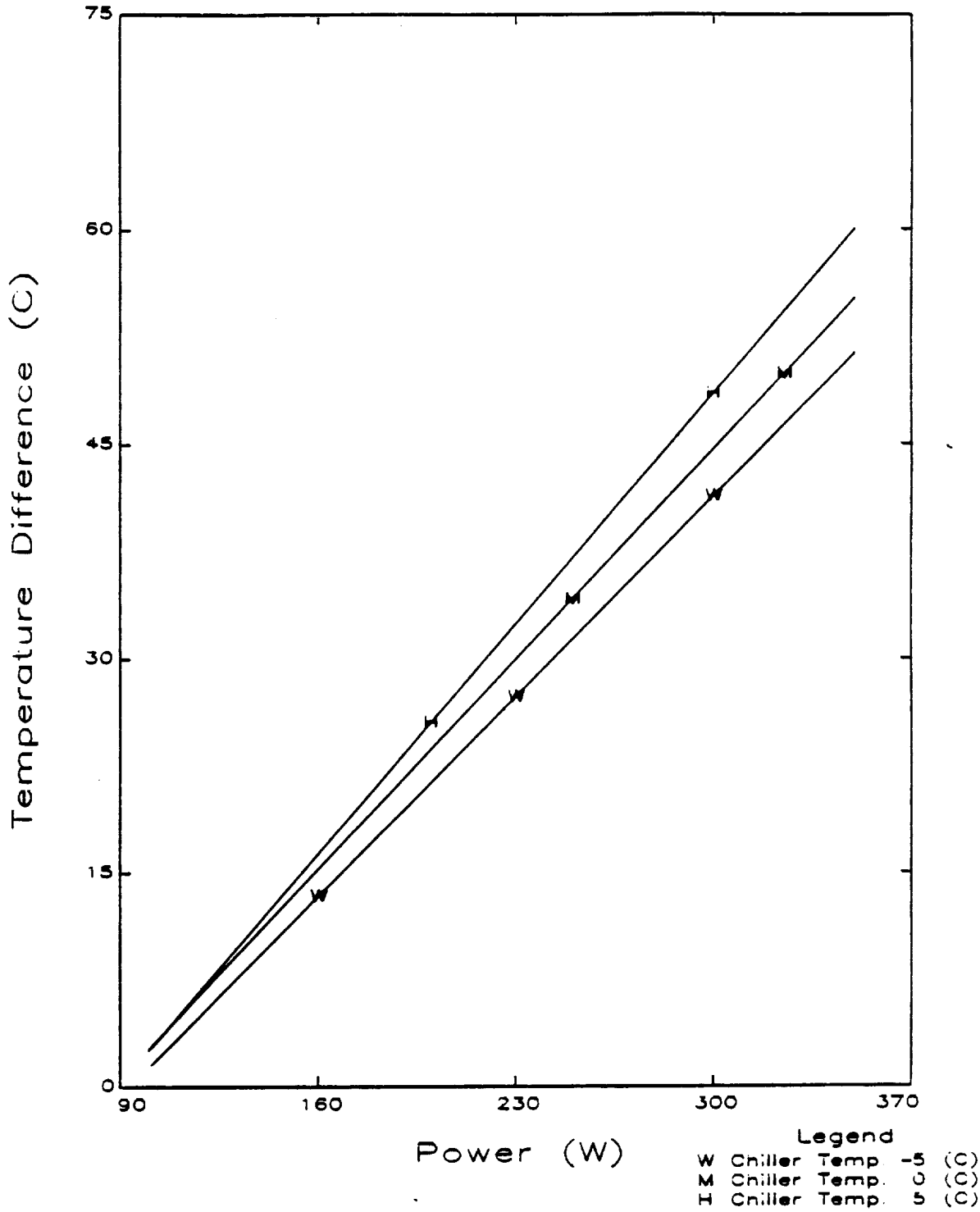

Fig. 18 - ΔT vs. Power Plot for Center Surface Temperatures of Evaporator #2 for Different Chiller Temperatures and at Mass Flow Rate of 0.7 (l/min)

- At a given time, the evaporator heating surface temperature is uniform at some average value
- Heat transfer rate from the evaporators towards the condenser can be represented by an exponential function of time
- Transient behavior is caused by applying a step power input to the evaporators, and the variation of temperature in time was recorded until a steady state was reached.

Using these assumptions, integration of the energy equation for the entire CPL model gives time variation of the evaporator temperature in terms of system parameters.

Details of the transient analysis is given in Appendix B. Equation (9) in this appendix gives transient evaporator wall temperature following a step increase in the power input to the evaporators. Transient temperature T_e is given in terms of the initial and final steady state evaporator temperatures and T_o,T_2 , and a time constant B. This parameter is given in terms of T_o , T_2 , and heat capacity of the evaporator and value of the power input at the final steady state.

Furthermore, Appendix B includes another analysis to predict effects of the inlet sub-cooling on the steady state evaporator temperature.

As discussed in detail in Appendix B, predictions of these analyses were compared with the test data collected by using the bench-top CPL test system. Good agreement has been obtained between the predicted and the measured temperature variations in time. The expression developed for predicting the inlet sub-cooling effects on the evaporator temperature was found to predict these effects at least in a qualitative way.

7. CONCLUSIONS AND RECOMMENDATIONS

- Critical evaluation of rather limited test data as well as predictions obtained from analysis of a model of CPL evaporator inlet section seems to indicate that anomalies in the transient CPL behavior, such as oscillatory temperature variations, are design-oriented rather than caused by standard operational procedures. It is expected that with proper CPL design, the mentioned oscillatory transient trends can be prevented.

The analytical study given in Appendix A identifies the important design parameters and presents a design criterion to be used, at least in a qualitative way, to obtain the proper design conditions which would help to avoid the undesireable oscillatory temperature behavior. No doubt, further study is recommended for better understanding of this rather

interesting, yet undesirable, transient phenomenon.

- Use of a reasonably simple bench-top CPL test heat pipe offered rather attractive possibilities for studying internal thermal-fluid dynamic operational characteristics of this system. It facilitated visual observations, as well as variation of most of the parameters controlling the transient operation. It was evident that the bench-top test CPL could achieve normal operation after a suddenly applied heat load. Tests indicated a significant influence of the inlet sub-cooling on the CPL performance.

The bench-top CPL used in the present investigation had a number of design limitations, such as condenser size, maximum capacity of the electric heaters, wick design, etc. It is recommended to conduct further tests by changing some of the design parameters of the bench-top CPL, and study effects on the performance. This test system offers design flexibility to facilitate such changes.

- The lumped-heat-capacity analytical CPL model developed in this study allows prediction of the transient response of the CPL test system. Good agreement has been obtained between the predicted and the measured temperature date. It is believed that the bench-top CPL and the model

developed for this system can be used to investigate qualitatively transient characteristics of more elaborate CPL heat pipes. In this sense, such research efforts supplement the more detailed quantitative information obtained by using the available computer programs that model the CPL heat pipe systems.

REFERENCES

1. McCabe, Jr., M.E., Ku J. and Benner, S., **"Design and Testing of a High Power Spacecraft Thermal Management System,"** NASA Technical Memorandum 4051, June 1988

2. Schweickart, R.B., Neiswanger, L., and Ku, J., **"Verification of an Analytical Modeler for Capillary Pump Loop Thermal Control Systems,"** AIAA-87-1630, AIAA 22nd Thermophysics Conference, Honolulu, Hawai, June 1987.

3. Boure, J.A., Bergles, A.E., and Tong, L.S., **"Review of Two-Phase Flow Instability,"** Nuclear Engineering and Design, Vol. 25, 1973, pp 165-192

4. Dynatherm Corporation, **"Final Report for Capillary Heat Transport Systems,"** DTM-0218-1101, Prepared for National Aeronautics and Space Administration, Goddard Space Flight Center, October 1985.

5. Dynatherm Corporation, **"Final Report for Hybrid Capillary/Mechanically Pumped Loop Evaluation and Test,"** DTM 0232-1100, Prepared for TSI Infosytems, October 1986.

PREV. ANN. 89A53264

APPENDIX A

Exploratory Study of Temperature Oscillations Related to Transient Operation of A Capillary Pumped Loop Heat Pipe

EXPLORATORY STUDY OF TEMPERATURE OSCILLATIONS RELATED TO TRANSIENT OPERATION OF A CAPILLARY PUMPED LOOP HEAT PIPE

A. M. Kiper
The George Washington University
Washington, D. C.

T. D. Swanson and R. McIntosh
NASA Goddard Space Flight Center
Greenbelt, Maryland

ABSTRACT

An analytical study has been conducted for better understanding of a peculiar transient behavior which was displayed in testing of a Capillary Pumped Loop (CPL) heat pipe system. During several test runs of this CPL system varying degrees of surface temperature oscillations occurred in the inlet line of the evaporators. Although several theories have been forwarded to explain this observed phenomenon, a satisfactory understanding of causes of these oscillations is still missing. The present investigation derives the conditions which lead to such oscillatory temperature behavior in evaporator inlet section of the mentioned CPL system. Stability characteristics of these temperature oscillations were investigated.

NOMENCLATURE

- A = cross sectional area of inlet pipe wall
- c = specific heat
- d = pipe inside diameter
- f = frequency
- $\bar{f}$ = dimensionless frequency
- h = convective heat transfer coefficient
- i = $\sqrt{-1}$, imaginary unit
- k = thermal conductivity
- $\bar{m}$ = $(hP/kA)^{1/2}$
- m = $\bar{m}\,d$, dimensionless
- M = mass of the evaporator body
- $\bar{M}$ = $(Mc\alpha)/kAd$, dimensionless
- P = πd, pipe perimeter
- Q = rate of heat transfer from the evaporator to the condenser
- Q_e = rate of heat flow to the evaporator
- Q_2 = steady state value of Q_e
- Q_p = heat conduction to the inlet liquid piping
- $\bar{Q}_2$ = $(Q_2 d)/kA\Delta T_o$, dimensionless
- q = $\left(s + m^2\right)^{1/2}$, dimensionless
- s = complex variable
- T = pipe wall temperature
- T_e = uniform evaporator shell temperature
- T_2 = steady state value of T_e
- T_o = steady state temperature at $x = 0$
- T_∞ = liquid temperature at inlet pipe
- W = power input to the evaporator section
- $\bar{W}$ = $(Wd)/(kA\Delta T_o)$, dimensionless
- $\bar{x}$ = distance shown in Fig. 3
- x = $\bar{x}/d$, dimensionless distance
- z = $u \pm iv$, complex variable
- α = thermal diffusivity $(k/\rho c)$
- ΔT_o = $T_o - T_\infty$
- λ = $\beta + i\eta = z - m^2$, Fig. 4
- θ = $(T - T_\infty)/(T_o - T_\infty)$, dimensionless temperature
- ρ = density
- $\bar{\tau}$ = time
- τ = $(\alpha\bar{\tau}/d^2)$, dimensionless time

INTRODUCTION

NASA-Goddard Space Flight Center's ongoing Space Station thermal management program includes development and testing of several CPL engineering models. As described in Ku et al. (1), in the closed loop CPL system working liquid is transported from the condenser to the

evaporator via the liquid piping under the capillary pressure developed in the evaporators. A special high density polyethylene wicking material used in the evaporators provides the ability to transfer large heat loads over long distances without the need for a pump to circulate the working fluid. The working fluid is drawn through the wick into the evaporator where it vaporizes. Heat is removed from the working fluid in the condenser where the vapor is condensed back to a liquid. A schematic of this process is shown in Fig. 1. The purpose of the isolators in this figure is to thermally decouple and prohibit vapor back flow among the individual evaporator pumps. Vapor back flow may otherwise occur if one evaporator overheats (due to a variety of reasons) and loses its liquid prime.

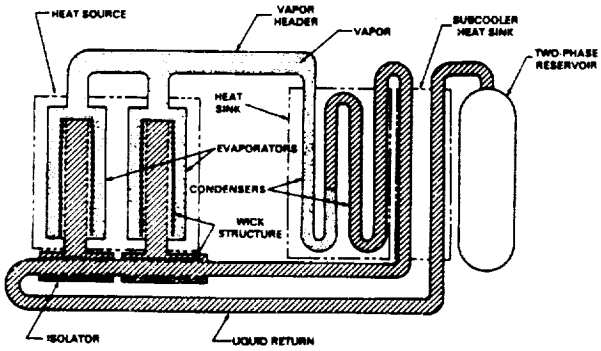

Figure 1. CPL Functional Schematic

The CPL test program included experiments of four different CPL systems. Ku et al. (2) noted that these tests demonstrated the ability of a CPL system to operate over a wide range of conditions and thus established viability of these systems for high power thermal management of large spacecraft, such as the NASA Space Station. During assessment of the CPL-2 test data, however, a rather unexpected phenomenon was observed. This test system displayed temperature oscillations in the inlet line and the isolator for each of the evaporator pumps. As shown in Fig. 2., temperature fluctuations were most prominent at heat loads between 300 and 500 watts for each evaporator pump. Experiments have shown that the inlet line fluctuations were the most volatile, and that unexpected pump deprimes frequently occurred at low power level changes. A typical low heat load pump deprime was usually preceded by fluctuations in that pump's inlet temperature. Each pump had a unique frequency and amplitude for its inlet and isolator temperature fluctuations. Typical amplitude and period of the observed temperature fluctuations were about 2 ^{o}C and 3 minutes.

Whatever the cause of the temperature fluctuations recorded in the inlet line of the CPL-2 evaporators, testing of the other CPL systems to date has not resulted in similar observations. Although several theories have been forwarded to explain this observed phenomenon, a satisfactory understanding of causes of these fluctuations is still lacking. It is well known that thermally induced oscillations can introduce operational problems in two-phase flow systems if they lead to flow or temperature instabilities, Boure et al. (3). Therefore, it is evident that reliable operation of the CPL system necessitates understanding of characteristics of the observed temperature fluctuations as well as conditions of stability of such fluctuations. This, in turn, necessitates a rather complete study of the CPL System dynamics.

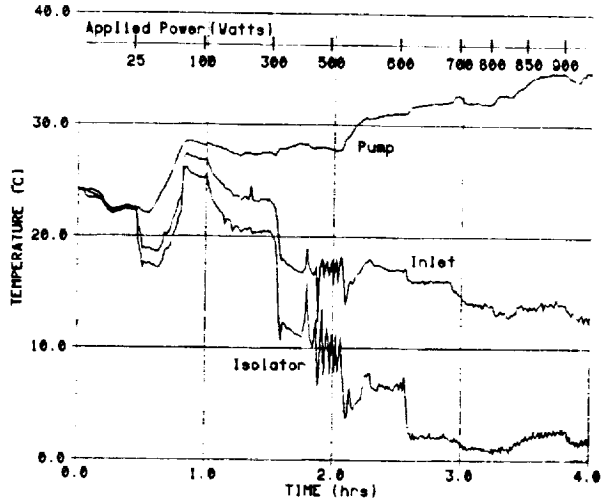

Figure 2 - CPL 2 Test Data

Although the subject of transient heat pipe behavior has received considerable recent attention, the studies dealt mainly with simple, single tube-container heat pipes which do not have the CPL system type fluid flow characteristics, Beam (4). Because of possible existence of two-phase flow conditions, the CPL system operation could involve thermally induced two-phase flow instabilities. Considering the wide spectrum of various types of static and dynamic two-phase flow instabilities, a rather complete study of the CPL system dynamics is very difficult. Therefore, the present exploratory study is an attempt to introduce a reasonably simple mathematical model which can be used to explain, at least in qualitative way, characteristics of the temperature fluctuations observed in the CPL-2 tests.

A recent study by Colwell and Chang (5) concluded that transient normal heat pipe operation can be predicted accurately by using the transient heat conduction equations applied to the heat pipe shell and to the combination fluid capillary structure with appropriate initial and boundary conditions. It was also noted that under adverse conditions, account must be taken of internal fluid dynamics and predictions become much more difficult.

It is expected that the design differences between the simple, single tube-container heat pipe and the CPL system would lead to different transient behavior of these systems. If, however, one assumes a quasi-steady state fluid mechanics, the conclusion noted by Colwell and Chang can be used to define a simple mathematical model of the CPL evaporator pump for the purpose of studying the temperature variations in this section of the CPL System. The present study reformulates the energy balance of the CPL evaporator as an initial and boundary-value

problem. The governing differential equation is solved for the inlet pipe wall temperature of evaporator by the method of the Laplace transformation and use of the Inversion Theorem. This approach is convenient for determining the conditions which would cause the oscillatory temperature behavior. A preliminary stability criterion is developed for investigating characteristics of these oscillations. Comparison of the present analytical work with the experimental results has been done for one limited case, only. Assessment of the large amount of CPL test data is still in progress. Extension of the present analytical work and comparison of its results with the CPL test data are planned for the near future.

FORMULATION

Figure 3 shows a schematic diagram of the model of the CPL evaporator inlet section used for the analysis. The heat conduction rate from the evaporator to the inlet piping, Q_p, is partly stored in the piping and partly removed by convection by the liquid entering the evaporator.

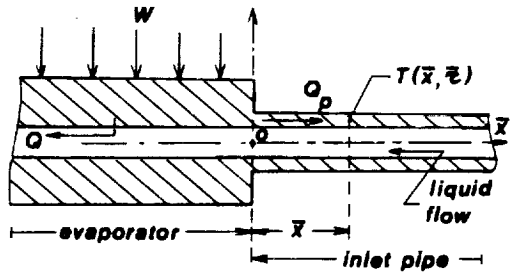

Figure 3 — Model of CPL Evaporator Inlet Section

Regarding the inlet piping section as essentially a one-dimensional configuration, the pipe wall temperature as a function of position, $\bar{x}$, and time, $\bar{\tau}$, will satisfy the equation

$$\frac{\partial^2 T}{\partial \bar{x}^2} - \bar{m}^2(T - T_\infty) - \frac{1}{\alpha}\frac{\partial T}{\partial \bar{\tau}} = 0 \qquad (1)$$

This equation assumes that outside surface of the inlet pipe section is adiabatic. The boundary and initial conditions are given by

$$\bar{\tau} = 0 \quad , \quad T = T_\infty \qquad (2)$$

$$\bar{x} \to \infty \quad , \quad T = T_\infty \qquad (3)$$

$$\bar{x} = 0 \quad , \quad \frac{\partial T}{\partial \bar{x}} = -\frac{Q_p}{kA} \qquad (4)$$

The magnitude of Q_p may vary in time until the system is brought to a steady state at a desired operating heat input to the evaporator pump. Although the length of the inlet pipe is finite, boundary condition (3) is plausible since, the cross-sectional area of the pipe wall is very small compared to the length of the inlet pipe, Kreith (6). The heat conduction rate Q_p will be determined later by considering the energy balance of the evaporator pump.

In terms of the nondimensional variables θ, m, x, and τ, Eq. (1) and conditions (2-4) become,

$$\frac{\partial^2 \theta}{\partial x^2} - m^2\theta - \frac{\partial \theta}{\partial \tau} = 0 \qquad (5)$$

$$\tau = 0 \qquad \theta = 0$$

$$x \to \infty \qquad \theta = 0 \qquad (6)$$

$$x = 0 \qquad \frac{\partial \theta}{\partial x} = F(0,\tau)$$

Taking the Laplace transform with respect to dimensionless time τ, the transformed equation and associated boundary conditions are

$$\frac{d^2\bar{\theta}}{dx^2} - q^2\bar{\theta} = 0 \qquad (7)$$

$$x \to \infty \qquad \bar{\theta}(\infty, s) = 0 \qquad (8)$$

$$x = 0 \qquad \frac{d\bar{\theta}}{dx} = F_1(0,s)$$

where $q^2 = s + m^2$, and s is a complex variable.

The boundary condition at $x = 0$ is determined by considering the energy balance of the evaporator

$$-kA\left.\frac{\partial T}{\partial \bar{x}}\right|_{\bar{x}=0} = W - Q - Mc\frac{\partial T_e}{\partial \bar{\tau}} \qquad (9)$$

where, at $\bar{x} = 0$ the inlet pipe wall temperature, T, and the evaporator temperature, T_e, are equal. In this equation heat loss to the ambient from the well insulated evaporator is neglected. Assuming that the evaporator temperature T_e is uniform along the evaporator length,

$$\frac{\partial T_e}{\partial \bar{\tau}} = \left.\frac{\partial T}{\partial \bar{\tau}}\right|_{\bar{x}=0} \qquad (10)$$

The initial temperature of the heat pipe is assumed to be T_∞. It is also assumed that startup consists in introducing a heat flow Q_e uniformly distributed over the length of the evaporator which is variable during the startup time until the pipe goes into the steady-state regime with temperature T_2 and heat flow Q_2.

It was shown by Cotter (7) that for all reasonable heat pipe startup programs $Q_e(\tau)$ will be between two extreme cases: (i) the slow startup in which Q_e increases from 0 to Q_2 so slowly that the heat pipe passes through a sequence of essentially steady states; and (ii) the fast startup for which $Q_e = 0$ for $\tau < 0$, and $Q_e = Q_2$ for $\tau > 0$. When the ambient temperature T_∞ is greater than the lowest temperature at which continuum flow can be established the startup becomes uniform. Under these conditions, for a slow startup heat transfer from the evaporator to the condenser is given by the linear relation

$$Q = Q_2(T_e - T_\infty) / (T_2 - T_\infty) \tag{11}$$

where,

$$T_e = T\Big|_{\bar{x}=0} \text{ and } T_2\Big|_{\bar{x}=0} = T_o \tag{12}$$

A similar linear equation with a constant term will hold in the case of rapid startup. Since the constant term will not affect results of the present analysis, Eq. (11) is used in the following derivations. Substituting Eqs. (10-12) into (9),

$$\left(- kA \frac{\partial T}{\partial \bar{x}} + Mc \frac{\partial T}{\partial \bar{\tau}} + Q_2 \frac{T-T_\infty}{T_2-T_\infty}\right)_{\bar{x}=0} = W \tag{13}$$

In terms of nondimensional variables this equation becomes,

$$\left(- \frac{\partial \theta}{\partial x} + \bar{M} \frac{\partial \theta}{\partial \tau} + \bar{Q}_2\theta\right)_{x=0} = \bar{W} \tag{14}$$

This equation provides $F(0,\tau)$ in the boundary condition Eq. (6)

$$F(0,\tau) = \frac{\partial \theta}{\partial x}\Big|_{x=0} = \left[\bar{M} \frac{\partial \theta}{\partial x} + \bar{Q}_2\theta\right]_{x=0} - \bar{W} \tag{15}$$

The Laplace transform of Eq. (14) becomes

$$\left(- \frac{d\bar{\theta}}{dx} + \bar{M}s\bar{\theta} + \bar{Q}_2\bar{\theta}\right)_{x=0} = \frac{\bar{W}}{s} \tag{16}$$

Referring to Eq. (8), $F_1(0,s)$ is determined from Eq. (16) by

$$F_1(0,s) = \frac{d\bar{\theta}}{dx}\Big|_{x=0} = \left[\bar{M}\, s\, \bar{\theta} + \bar{Q}_2\, \theta\right]_{x=0} - \frac{\bar{W}}{s} \tag{17}$$

Since in all cases θ and thus $\bar{\theta}$ is to be bounded as $x \to \infty$, solution of transformed Eq. (7) satisfying this boundary condition is given as

$$\bar{\theta} = A\, e^{-qx} \tag{18}$$

Substituting Eq. (18) into (16) gives A, and we get finally

$$\bar{\theta} = \frac{\bar{W} e^{-qx}}{s(q + \bar{M}s + \bar{Q}_2)} \tag{19}$$

By applying the Inversion Theorem to Eq. (19) we get

$$\theta = \frac{\bar{W}}{2\pi i} \int_{\gamma-i\infty}^{\gamma+i\infty} \frac{e^{\lambda\tau} \cdot e^{-\left(\lambda+m^2\right)^{1/2}x}}{\lambda\left[\left(\lambda+m^2\right)^{1/2} + \bar{M}\lambda + \bar{Q}_2\right]}\, d\lambda \tag{20}$$

Substituting $\lambda + m^2 = z$ and $d\lambda = dz$

$$\theta = \frac{\bar{W}}{2\pi i} \int_{\gamma-i\infty}^{\gamma+i\infty} \frac{e^{\left(z-m^2\right)\tau} \cdot e^{-z^{1/2}x}}{\left(z-m^2\right)\left[z^{1/2}+\bar{M}(z-m^2)+\bar{Q}_2\right]}\, dz \tag{21}$$

Substitution of $\lambda + m^2 = z$ is equivalent to a shift of origin to the point $\lambda = -m^2$ on the real β axis in the complex λ-plane. In doing this neither the contour of integration nor the positions of the singularities are affected in relation to each other, so the transformation can be made without any alteration in the integration technique.

The integrand of Eq. (21) has a branch point at $z = 0$. Its poles are at $z = m^2$ and at the roots of

$$z^{1/2} + \bar{M}(z - m^2) + \bar{Q}_2 = 0 \tag{22}$$

All poles are to the left of the line $\beta = \gamma$ in the λ-plane.

To evaluate the integral in Eq. (21) we choose a suitable contour which is equivalent to Br_1, as shown in Fig. 4. The contour has a cut along the negative real axis so that the integrand is a single-valued function of z within and on the contour. In the limit as the radius of the large circle tends to infinity the line integral (21) is replaced by integrals along CD and EF together with contributions from the small circle at origin of the complex z-plane and any poles of the integrand.

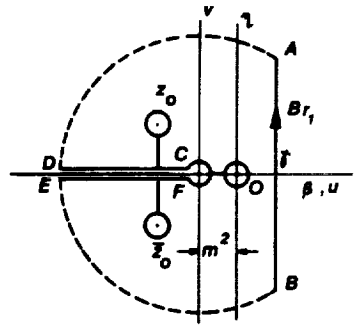

λ – plane (β,η) z – plane (u,v)

Figure 4 – Contour for the Complex Integral

It was noted by Arpaci (8) that the contribution to transient temperature change by a simple pole of the Inversion Theorem may be interpreted in physical terms by considering the location of this pole on the complex plane. The contribution of a simple pole at the origin is a steady term. On the imaginary axis, the contribution is a periodic term with constant amplitude. With poles located on the half plane to the left of the imaginary axis, the contribution is a periodic term with decaying amplitude. If the pole lies to the right of the imaginary axis, the contribution to the solution becomes unstable.

Therefore, in the present analysis, the oscillatory component to the temperature will be contributed by appropriate poles at the roots of Eq. (22). In the following discussion only this contribution is considered.

To find the oscillatory contribution to the temperature we evaluate Eq. (21) at the two poles $z_o = u_o \pm iv_o$ round the circles shown in Fig. 4 where z_o are the conjugate roots of Eq. (22). Let $Res_1(z_o)$ and $Res_2(\bar{z}_o)$ denote residues of the integrand in Eq. (21) at these two poles. Then, according to the Cauchy's residue theorem contributions of these poles to the integral in Eq. (21) is

$$2\pi i \left[Res_1(z_o) + Res_2(\bar{z}_o)\right] \tag{23}$$

where, $Res_1(z_o)$ and $Res_2(\bar{z}_o)$ are conjugate functions. The residue at the pole $z_o = u_o + iv_o$ is given by

$$Res_1(z_o) = \bar{W}\left[\frac{e^{\left(z-m^2\right)\tau} \cdot e^{-z^{1/2}/\bar{X}}}{\frac{d}{dz}\left\{\left(z-m^2\right)\left[z^{1/2} + \bar{M}(z-m^2) + \bar{Q}_2\right]\right\}}\right]_{z=z_o}$$

$$= \bar{W}\frac{e^{\left(z_o-m^2\right)\tau} \cdot e^{-z_o^{1/2}/\bar{X}}}{\left(z_o-m^2\right)\left(\bar{M}+0.5z_o^{-1/2}\right)} \tag{24}$$

Therefore, the oscillatory contribution to the temperature becomes

$$\theta_\omega = Res_1(z_o) + Res_2(\bar{z}_o) \tag{25}$$

$Res_2(\bar{z}_o)$ is obtained by writing -i for i in Eq. (24).

Substituting $z_o = u_o + iv_o$ into Eqs. (23 and 24) and using the Euler's formula $e^{iv_o} = \cos v_o + i \sin v_o$, Eq. (25) is reduced to the following form

$$\theta_\omega = 2\bar{W}e^{(u_o-m^2)\tau} \cdot e^{-\mu x}\cos(v_o\tau - \psi x - \phi) \tag{26}$$

where, μ and ψ are given, in terms of u_o and v_o, by the equations

$$\mu^2 = 0.5\left[\left(u_o^2 + v_o^2\right)^{1/2} + u_o\right]$$

$$\psi^2 = 0.5\left[\left(u_o^2 + v_o^2\right)^{1/2} - u_o\right] \tag{27}$$

The phase constant $\phi = \tan^{-1}(Y/X)$ is obtained by determining X and Y from the equation

$$X + iY = \left(\mu^2 - 2i\mu\psi + \psi^2 - m^2\right)\left[\bar{M} + 0.5\,\frac{\mu - i\psi}{\mu^2+\psi^2}\right] \tag{28}$$

Equation (26) has the same form of the transient temperature variation obtained by Carslaw and Jaeger (2) for a problem related to systems for automatic temperature control. Therefore, in the present study, the oscillatory temperature contributions are evaluated in a way similar to that followed by these authors.

Roots of Eq. (22) are given by

$$z_o = u_o \pm iv_o = \frac{1}{2\bar{M}^2}\left(a \pm \sqrt{b}\right) \tag{29}$$

where,

$$a = 2m^2\bar{M}^2 - 2\bar{M}\bar{Q}_2 + 1$$

$$b = 1 + 4m^2\bar{M} - 4\bar{M}\bar{Q}_2 \tag{30}$$

and

$$u_o = m^2 + \frac{0.5}{\bar{M}^2} - \frac{\bar{Q}_2}{\bar{M}} \tag{31}$$

Temperature oscillations occur under conditions which make b in Eq. (29), negative

$$1 + 4m^2\bar{M} - 4\bar{M}\bar{Q}_2 < 0$$

or,

$$\bar{M}\bar{Q}_2 > m^2\bar{M} + 0.25 \tag{32}$$

With $b < 0$, v_o in Eq. (29) is given by

$$v_o = \frac{1}{\bar{M}^2}\left[\bar{M}\bar{Q}_2 - m^2\bar{M} - 0.25\right]^{1/2} \tag{33}$$

Then, referring to Eq. (26), the following cases can be considered:

(a) With $u_o - m^2 = 0$, the exponential term in Eq. (26) becomes unity. This case, therefore, corresponds to a steady maintained temperature oscillation. By using Eq. (31), this case occurs when

$$\bar{Q}_2 \cdot \bar{M} = 0.5 \tag{34}$$

(b) For $u_o - m^2 < 0$, or $\bar{M} \cdot \bar{Q}_2 > 0.5$, temperature oscillations are damped since, $\exp(u_o - m^2)\tau$ term in Eq. (26) decreases with increasing time τ.

(c) When $u_o - m^2 > 0$, temperature oscillations become unstable. In view of the condition given by (32), range of $\bar{M}\bar{Q}_2$ for unstable temperature oscillations is given by

$$m^2\bar{M} + 0.25 < \bar{M}\bar{Q}_2 < 0.5 \tag{35}$$

Referring to Eq. (26), the dimensionless frequency of the oscillations, $\bar{f}$, is given by $v_o = 2\pi\bar{f}$. Then, from Eq. (33)

$$\bar{f} = \frac{v_o}{2\pi} = \frac{\left[\bar{M}\bar{Q}_2 - m^2\bar{M} - 0.25\right]^{1/2}}{2\pi\bar{M}^2} \tag{36}$$

Since the time in seconds, τ, and the dimensionless time, $\bar{\tau}$, are related by $\tau = (\alpha\bar{\tau}/d^2)$, then the real frequency in seconds is given as

$$f = \frac{v_o}{2\pi} \cdot \frac{\alpha}{d^2}, \quad 1/\text{sec.} \tag{37}$$

In view of the expression (32), and Eq. (35), oscillatory frequency is always positive. The frequency range for the unstable oscillations will be determined by expression (35) and Eq. (36). Referring to the condition given by

(32), no oscillatory temperature behavior will be observed if,

$$\bar{M}\,\bar{Q}_2 < m^2\,\bar{M} + 0.25$$

or,

$$\bar{Q}_2 < m^2 + \frac{0.25}{\bar{M}} \qquad (38)$$

Substituting the expressions for m^2, $\bar{M}$ and $\bar{Q}_2$ this condition becomes

$$Q_2 < \left[hPd + 0.25\,\frac{(kA)^2}{Mc\alpha}\right]\Delta T_o \qquad (39)$$

Therefore, when the steady state rate of heat flow to the evaporator, Q_2, remains below the critical value given by (39), the inlet pipe and the evaporator wall temperatures will not include oscillatory terms. So far as the oscillatory temperature behavior is concerned, the critical operating range is given by (35). Within this range, oscillations become unstable. Outside this range either they do not exist, or are damped with the increasing time.

RESULTS AND DISCUSSION

Within the limitations of the one dimensional physical model used and the assumptions made on the CPL evaporator pump energy exchange characteristics, a solution was obtained representing the conditions which could cause an oscillatory contribution to the transient wall temperature variation in the inlet section of the CPL evaporator pump. Stability characteristics of these temperature oscillations were investigated and a preliminary stability criterion was introduced. To illustrate the utilization of the results contained in the present exploratory study, reference is made to the CPL-2 test data shown in Fig. 2. This figure exhibits rather prominent inlet pipe and isolator wall temperature fluctuations at evaporator heat loads between 300 and 500 watts. The frequency of these slow and rather steady oscillations was approximately 0.005 per second. When the heat load was increased to 500 watts oscillations were diminished. Although at higher heat loads small amplitude fluctuations were observed, these were attributed to cycling effects of the condenser chiller temperature controller. Above 900 watts, evaporator pump started to warm up indicating the beginning of a dry-up. It was observed that the inlet line oscillations were the most volatile, and that unexpected pump deprimes frequently occurred at low heat load changes. One of the major design differences between the CPL-2 and the other CPL test systems was at the evaporator pump inlet section. The CPL-2 inlet section included a multi-component brazing section which connected the aluminum evaporator shell to a stainless steel inlet tubing. It is suspected that this design enhanced the possibility of boiling and non-condensible gas accumulation in the inlet section. The other CPL test systems utilized straight aluminum inlet tubing welded to evaporator inlets.

Discussion of detailed design specifications of the CPL systems, assessment of the large amount of CPL test data, and comparison of results of the present study with this data are beyond the scope of the present investigation. Such a work is now in progress and will be reported later. The following discussion, however, summarizes conclusions of the present study related to performance of the CPL-2 test system.

The expression (39) implies that at a given steady-state heat flow, Q_2, larger values of parameters h, d, kA and ΔT_o and smaller values of $Mc\alpha$ would help in preventing occurrence of the temperature oscillations. Therefore, the evaporator liquid inlet sections having large diameters and wall thicknesses and made of materials of high thermal conductivities are better for preventing the temperature oscillations. The same is true for large h values. For this reason, a significant decrease in h caused by liquid bubbling or accumulation of non-condensible gases in the inlet section could lead to temperature oscillations. Therefore, the inlet section of the CPL-2 test system with its stainless steel piping and a multi-component brazing section would enhance occurrence of inlet section wall temperature oscillations. The situation is aggravated at low heat loads since, the low liquid flow rate helps initiation of the inlet boiling and non-condensible gas accumulation at the inlet section. Temperature difference ΔT_o is related to the liquid subcooling. Increase in ΔT_o would help to prevent the oscillations both directly in relation (39), and indirectly by preventing boiling in the inlet section.

Using the one-dimensional physical model to represent the inlet section of the CPL-2 system, following design parameters were determined:

d = 0.0127 m, stainless steel pipe diameter

(kA) = 0.128 W-m/deg C, equivalent value at the inlet to aluminum evaporator shell

M = 0.25 kg, mass of the aluminum evaporator shell

c = 896 J/kg-deg C, specific heat for the aluminum evaporator

α = 4×10^{-6} m^2/sec, thermal diffusivity of the stainless steel tubing

By using this information and equations given in the main text

$$\bar{M} = 0.55 \text{ and } \bar{Q}_2 = 0.0034\,Q_2$$

The condition for the steady oscillations is given by Eq. (34).

$$\bar{Q}_2 \cdot \bar{M} = 0.55(0.0034)Q_2 = 0.5$$

$$\therefore \quad Q_2 = 267.4 \text{ watts}$$

The total power input W, shown in Fig. 2, will be somewhat larger than Q_2. Since the steady temperature oscillations in this figure starts at 300 watts, the agreement between the analytical value and the test value seems to be adequate. Assuming that h and, therefore, m approaches zero in the inlet section, the frequency of oscillations is obtained from Eqs. (36 and 37)

$$\bar{f} = \frac{1}{2\pi(0.55)^2}\,[0.5 - 0.25]^{1/2} = 0.263$$

$$f = 0.263\,\frac{4 \times 10^{-6}}{(0.0127)^2} = 0.0065 \text{ 1/sec}$$

This value also agrees, as a first approximation, with the test value 0.005 1/sec. If h, therefore m, become large enough, then according to relation (38) no oscillatory behavior will occur.

ACKNOWLEDGEMENTS

This study was supported by the Goddard Space Flight Center, National Aeronautics and Space Administration, under Research Grant No. NAG 5-834, and the support is gratefully acknowledged.

REFERENCES

1. Ku, J. Kroliczek, E. J., Butler, D., Schweickart, R. B., and McIntosh, R., "Capillary Pumped Loop GAS and Hitchhiker Flight Experiments," AIAA-86-1249, AIAA/ ASME 4th Joint Thermophysics and Heat Transfer Conference, June 2-4, 1986.

2. Ku, J., Kroliczek, E. J., Taylor, W. J., and McIntosh, R., "Functional and Performance Tests of Two Capillary Pumped Loop Engineering Models," AIAA-86-1248, AIAA/ASME 4th Joint Thermophysics and Heat Transfer Conference, June 2-4, 1986.

3. Boure, J. A., Bergles, A. E., and Tong, L. S., "Review of Two-Phase Flow Instability," Nuclear Engineering and Design, Vol. 25, 1973, pp. 165-192.

4. Beam, J. E., "Transient Heat Pipe Analysis," Paper 85-0936, AIAA 20th Thermophysics Conference, June 19-21, 1985.

5. Colwell, G. T. and Chang, W. S., "Measurements of the Transient Behavior of a Capillary Structure Under Heavy Thermal Loading," Int. Heat Mass Transfer, Vol. 27, No. 4, 1984, pp. 541-551.

6. Kreith, F., Principles of Heat Transfer, 3rd ed., Intext Educational Publishers, 1973, pp. 58-59.

7. Cotter, T. P., "Heat Pipe Startup Dynamics," Proceedings of the Thermionic Conversion Specialist Conference, Oct. 30-Nov. 1, 1967, pp. 344-348.

8. Arpaci, V. S., Conduction Heat Transfer, 1st ed., Addison-Wesley Publishing Company, 1966, pp. 421-423.

9. Carslaw, H. S., and Jaeger, J. C., Conduction of Heat in Solids, 2nd ed., Oxford University Press, 1959, pp. 407-412.

PREV. ANN.
90A 38388

APPENDIX B

Transient Analysis of A Capillary Pumped Loop Heat Pipe

AIAA 90-1685

Transient Analysis of a Capillary Pumped Loop Heat Pipe

A. Kiper, G. Feric and M. Anjum
George Washington Univ.
Washington, DC
T. Swanson
NASA-Goddard
Greenbelt, MD

AIAA/ASME 5th Joint Thermophysics and Heat Transfer Conference

June 18-20, 1990 / Seattle, WA

TRANSIENT ANALYSIS OF A CAPILLARY PUMPED LOOP HEAT PIPE

A.M. Kiper*, G. Feric and M.I. Anjum*
The George Washington University
Washington, D.C.

T. D. Swanson*
NASA Goddard Space Flight Center
Greenbelt, Maryland

Abstract

A bench-top Capillary Pumped Loop (CPL) test system has been developed and tested to investigate the transient mode operation of this system by applying a step power input to the evaporators. Tests were conducted at several power input and evaporator inlet subcooling combinations. In addition, a lumped-heat-capacity model of the CPL test system has been presented which is used for predicting qualitatively the transient operation characteristics. Good agreement has been obtained between the predicted and the measured temperature variations. A simple evaporator inlet subcooler model has also been developed to study effects of inlet subcooling on the steady-state evaporator wall temperature. Results were compared with the test data collected.

Nomenclature

A	Heat transfer surface area
c	Specific heat
D	Inlet pipe outside diameter
d	Capillary wick thickness
h	Convective heat transfer coefficient
h_1, h_2	Inlet and exit enthalpies
k	Thermal conductivity
M	Mass of evaporator walls
$\dot{m}$	Evaporator fluid mass flow rate
$\dot{m}_1$	Subcooler coolant flow rate
Pr	Prandtl number
$\dot{Q}_e$	Evaporator input power
$\dot{Q}_2$	Steady state input power
$\dot{q}$	Subcooling rate per unit capillary wick volume
Re	Reynolds number
T	Temperature
T_e, T_2	Evaporator wall temperatures, transient and steady state
T_o	Initial evaporator wall temperature
T_s	Saturation temperature of the evaporator fluid
T_c	Temperature of the subcooled fluid
x	Position coordinate
β	Inverse of the time constant
θ	$(T_e - T_o)/(T_2 - T_o)$
τ	Time
τ_o	Time lag parameter

Introduction

Temperature control of large space structures, such as a Space Station, will require advanced heat acquisition and transport systems to keep on-board temperatures within their allowable ranges. Two-phase temperature control systems which utilize an evaporation-condensation cycle offer significant advantages for such applications. The Capillary Pumped Loop (CPL) heat pipe is a two-phase heat transport system which utilizes the surface tension forces developed in a fine pore capillary wick to circulate the working fluid.

The CPL test systems have exhibited up to an 8 kW heat load capacity over 10 meter transport distance in one-g environment.[1] Recent testing of the High Power Spacecraft Thermal Management (HPSTM) demonstration system has shown that in the capillary mode, the HPSTM evaporators can acquire a total heat load of between 600 W and 24 kW.[1] Testing of a small-scale CPL experiment aboard Space Shuttle verified the thermal control capability of this system in a microgravity environment.

A CPL system which is integrated into a system such as a spacecraft is expected to perform in a wide range of thermal environments of space. Therefore, an analyst may need to simulate and evaluate the operation of the CPL system under transient conditions. Although recently a computer model was developed to predict the steady state and transient behavior of a CPL system, there exists a need for both test data of the transient CPL operation, as well as a simple CPL model which can be used for evaluating this data.[2] Such a model would allow direct study of pertinent system parameters on the transient CPL operation.

This paper describes a specially designed bench-top CPL test system which was utilized to collect transient mode operation data by applying a step power input to the evaporators. Temperatures were measured at several power input and inlet subcooling combinations. In addition, a lumped-heat-capacity model of the CPL test system has been developed for predicting the transient operation characteristics. Comparisons of the analytical results with the test data are presented.

Importance of the evaporator inlet subcooling in stable CPL operation is well known. Test system of the present work allows qualitative investigation of some subcooling effects on the CPL performance.

*Member AIAA

Description of the Test System

A schematic of the bench-top CPL test system is shown in Fig. 1. It incorporates four evaporators, a reservoir, a condenser as well as measurement and data acquisition systems. Each evaporator, shown in Fig. 2, consists of a vertical Pyrex glass cylindrical chamber of 70 mm O.D. and 100 mm height. The brass plates enclose the chamber and the bottom plate is heated by a Chromalox electric disk heater of 350 W maximum capacity. The capillary wick consisting of two 100 mesh brass screen layers is pressed against the heated surface by using a top 8 mesh stainless steel screen piece and a spring combination. The capillary wick is manufactured in such a form that it extends into the vertical liquid inlet pipe in order to bring the liquid into the wick structure by capillary action. To improve the liquid distribution, an absorbent felt layer is placed between screen layers of the horizontal wick.

Pyrex glass evaporator chamber allows visual observation of the evaporator operation. Distilled water is used as the working fluid. Liquid coming to the evaporators is subcooled by using specially designed inlet subcoolers. Vapor leaves the evaporators through outlets located at the top plates. Cooling fluid to the double-pipe condenser is supplied by a Neslab Flowthru Cooler. Although major components of the test system are insulated, a significant portion of the evaporator heat input was lost during the experiment. These heat losses, however, may be of little importance since the purpose of the present study is not related to the thermal efficiency of the test CPL system but related to the transient operating characteristics.

The bench-top CPL test system has been tested to collect transient mode operation test data by applying a step power input to the evaporators. Temperatures were measured at several power input and inlet subcooling combinations. The evaporator temperature was plotted in dimensionless form until the steady state condition is reached.

Analyses

Transient Temperature Response

In transient operations of the CPL system, temperatures of various system components do not change uniformly. Therefore, the isothermal transient heat pipe models used in earlier studies cannot be used for predicting the transient thermal CPL performance. In the present investigation a lumped-heat-capacity model of the CPL system has been developed by assuming that

(i) At a given time, the evaporator heating surface temperature is uniform at some average value,

(ii) Heat transfer rate from the evaporators towards the condenser can be represented by an exponential function of time.

Referring to the simplified CPL model in Fig. 3, energy balance of the evaporator results in the following equation

$$\dot{Q}_e = \dot{m}\,(h_2 - h_1) + (Mc)_e \frac{dT_e}{d\tau} \qquad (1)$$

where, h_1 and h_2 inlet and exit enthalpies, $\dot{Q}_e$ rate of evaporator heat input, $\dot{m}$ rate of fluid flow, $(Mc)_e$ heat capacity of the evaporator and $dT_e/d\tau$ is the time rate of change of the uniform evaporator temperature. When the steady state is reached Eq. (1) becomes

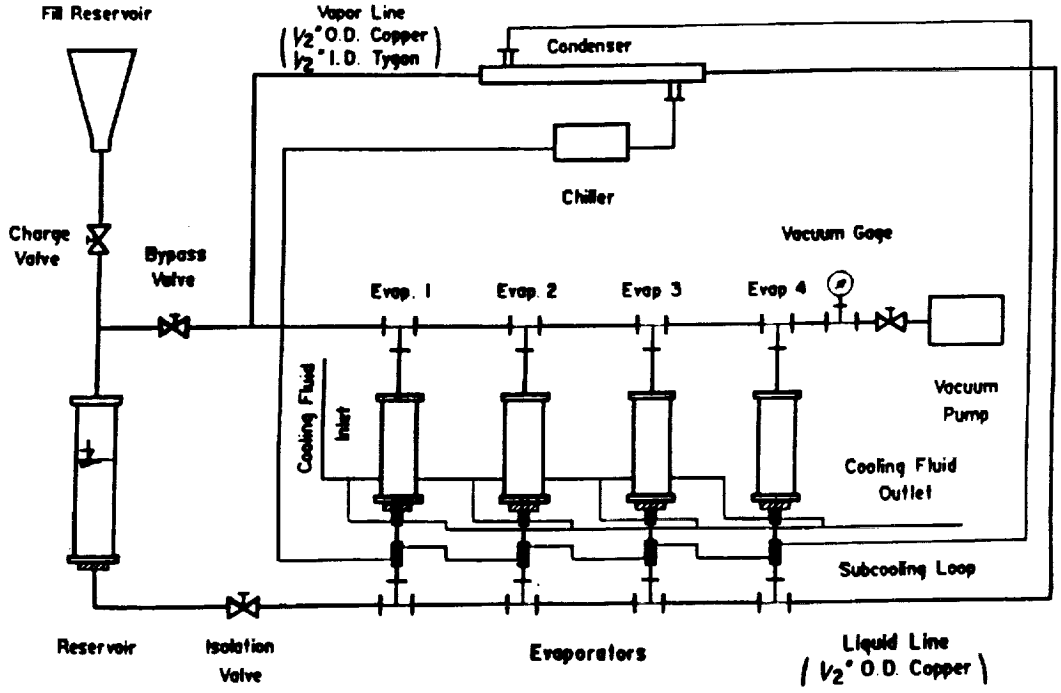

Fig. 1 - Schematic of the Bench-Top CPL Test System

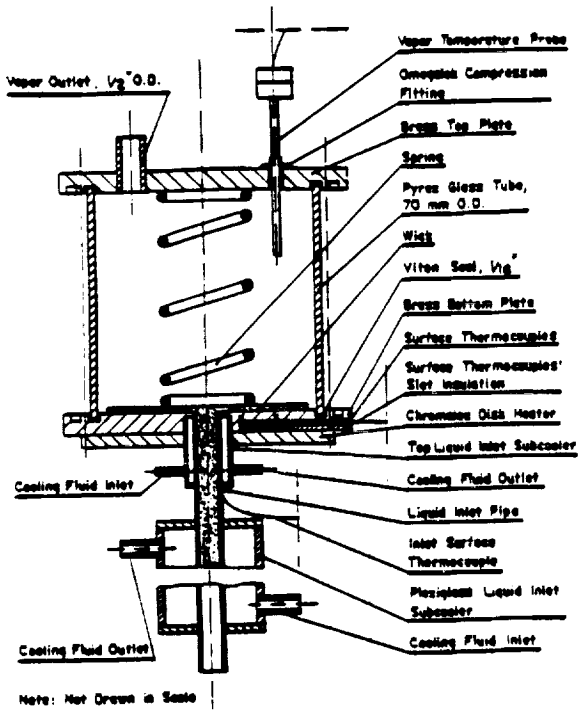

Fig. 2 - Drawing of One of the Evaporators

$$\dot{Q}_2 = \left[\dot{m}(h_2 - h_1)\right]_{st} \qquad (2)$$

where $\dot{Q}_2$ is the heat input under steady state conditions. It is assumed that time variation of $\dot{m}(h_2 - h_1)$ can be represented by an exponential function

$$\dot{m}(h_2 - h_1) = \dot{Q}_2\left[1 - e^{-\beta\tau}\right] \qquad (3)$$

Then, Eq. (1) becomes

$$\dot{Q}_e = \dot{Q}_2\left[1 - e^{-\beta\tau}\right] + (Mc)_e \frac{dT_e}{d\tau} \qquad (4)$$

If a sudden step power input $\dot{Q}_2$ is applied to the evaporator, $\dot{Q}_e = \dot{Q}_2$ for $\tau > 0$, and then Eq. (4) reduces to the following differential equation

$$\frac{dT_e}{d\tau} - \frac{\dot{Q}_2}{(Mc)_e} e^{-\beta\tau} = 0 \qquad (5)$$

Or, in non-dimensional form

$$\frac{d\theta}{d\tau} - Be^{-\beta\tau} = 0 \qquad (6)$$

where, $\theta = (T_e - T_o)/(T_2 - T_o)$; T_o, T_2 are initial and steady state evaporator temperatures and $B = \dot{Q}_2/(Mc)_e(T_2 - T_o)$. Integration of Eq. (6) from $\tau = 0$ to a final time τ gives,

$$\theta = \frac{B}{\beta}\left[1 - e^{-\beta\tau}\right] \qquad (7)$$

Dimensionless temperature ratio given in Eq. (7) becomes $\theta = 1$ when time assumes very large values.

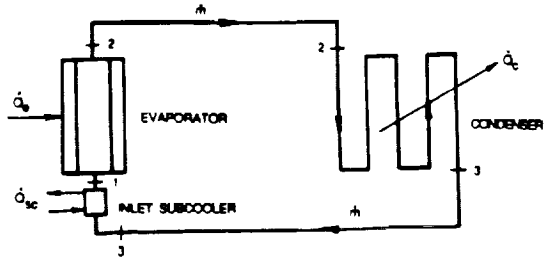

Fig. 3 - Simple CPL model for Thermal Analysis

This condition implies that value of inverse of the time constant is given by $\beta = B$. Then Eq. (7) reduces to

$$\theta = 1 - e^{-\beta\tau} \qquad (8)$$

Or, the variation of evaporator temperature T_e is given as

$$T_e - T_o = \left(T_2 - T_o\right)\left[1 - e^{-\beta\tau}\right] \qquad (9)$$

For a given evaporator power input and inlet subcooling, the value of $\beta = B$ will be known if the steady state evaporator temperature is determined experimentally.

Effects of Inlet Subcooling

Start up of the CPL system and its stable operation require a subcooling of the liquid entering the evaporator sections. The importance of inlet subcooling was emphasized in several experimental works.[3] Attempts to run the CPL system without local subcooling were unsuccessful. Once subcooling was added, performance improved dramatically. No study, however, is available which investigates effects of the evaporator inlet subcooling on the CPL performance. The analysis which follows investigates effects of the inlet subcooling on the steady state evaporator temperature. Since this temperature is the controlling parameter in time constant of Eq. (8), the analysis is also to describe the subcooling effect on the evaporator transient temperature variation.

The layer of wick immediately contacting the heating surface is saturated with liquid. The mechanism of heat transfer consists of heat exchange by conduction through the wetted capillary wick structure. This assumes that a good contact is maintained between the wick and the heating surface. The steady state capillary wick temperature variation in a direction normal to the heating surface can be obtained by assuming that effect of subcooled liquid flow is accounted for by using a heat conduction model with a uniform heat sink. Referring to portion of the screen capillary wick, shown in Fig. 4, temperature variation in x-direction is given by

$$\frac{d^2T}{dx^2} + \frac{\dot{q}}{k_e} = 0 \qquad (10)$$

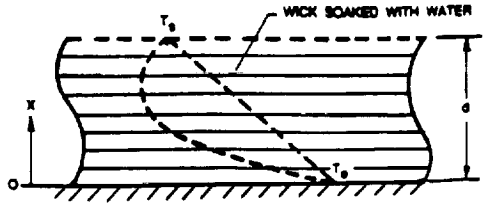

Fig. 4 - Portion of Horizontal Capillary wick

where, $\dot{q}$ represents uniform cooling rate of the wick structure by the subcooled liquid per unit volume of the capillary wick. Its value is given by $\dot{q} = -\dot{m}.c(T_s-T_c)/\text{Wick volume}$; where, $\dot{m}c(T_s-T_c)$ is subcooling rate of the liquid entering the evaporator, T_s and T_c are the saturation and the subcooled liquid temperatures, and k_e is the wetted wick thermal conductivity, respectively.

The wick temperature in x-direction changes from the steady state wall temperature T_2 to the vapor saturation temperature T_s at the liquid-vapor interface. Then the integration of Eq. (10) gives,

$$T(x) = (xd - x^2)\frac{\dot{q}}{2k_e} - \frac{T_w-T_s}{d}x + T_e \qquad (11)$$

where, d is thickness of the capillary wick. Steady state power input to the evaporator from the heated surface is given by

$$\dot{Q}_2 = -k_e A \left.\frac{dT}{dx}\right|_{x=0} \qquad (12)$$

where, A is the evaporator heat transfer surface area. By substituting (dT/dx) from Eq. (11) and, the expression for $\dot{q}$ into Eq. (12) one obtains

$$\dot{Q}_2 = 0.5\,\dot{m}c\,(T_s-T_c) + (k_eA/d)\,(T_2-T_s) \qquad (13)$$

This equation can be rewritten as

$$(T_2 - T_s) + \frac{d}{2k_eA}[\dot{m}c(T_s-T_c)] = \frac{\dot{Q}_2 d}{k_eA} \qquad (14)$$

This expression indicates that at constant power input $\dot{Q}_2$ and saturation temperature T_s, the evaporator temperature T_2 will decrease with increased inlet subcooling. In testing the bench-top CPL system, the steady state evaporator temperature T_2 was measured at different inlet subcooling rates at a given power input. Subcooling rate was controlled by changing the coolant flow rate in the inlet subcooler.

Fig. 5 shows a schematic of the evaporator inlet subcooler. Lower stem of the capillary wick fills the inlet pipe almost completely. Since the liquid flow rate to the evaporator is very small, wetted wick can be treated as a heat conduction medium. Heat from the subcooled liquid is conducted through the wick, and removed from outside surface of the inlet pipe by convection to coolant of the inlet subcooler. The rate of

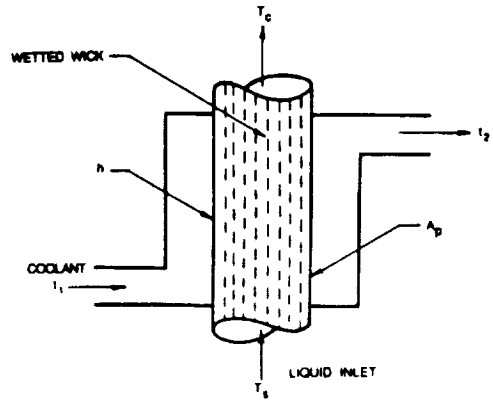

Fig. 5 - Schematic of the inlet Subcooler

subcooling is given by

$$\dot{Q} = \dot{m}\,c(T_s - T_c) = hA_p\,(\Delta T) \qquad (15)$$

where, A_p and h are the subcooler heat transfer surface area and the convective heat transfer coefficient. ΔT is the difference between the inlet pipe outside surface temperature and the subcooler coolant temperature. Since the coolant flow rate is much greater than the rate of liquid flow into the evaporator, ΔT remains almost constant at different coolant flow rates so long as the inlet temperatures of two fluids into the subcooler do not change. However, h in Eq. (15) varies with the coolant flow rate $\dot{m}_1$. Consequently, the rate of evaporator inlet liquid subcooling changes with $\dot{m}_1$.

Considering the subcooler design used in the bench-top test system, the coolant flow can be treated as a flow across a heated pipe. Then the average heat transfer coefficient h can be calculated by using the following equation,[4]

$$\frac{hD}{k_c} = C\,(Re)^n \cdot Pr^{1/3} \qquad (16)$$

Coefficients C and n are given in terms of the Reynolds number based on the outside diameter of the inlet pipe (D). Since temperature of the coolant changes very small amount during the subcooling process, physical properties in Eq. (16) can be treated as constant. Also noting that the (Re) can be expressed in terms of the coolant flow rate $\dot{m}_1$, then, Eq. (16) can be rewritten as

$$h = C(N)(\dot{m}_1)^n \qquad (17)$$

where, N is a known constant. Substituting Eqs. (15) and (17) into Eq. (14), one obtains,

$$(T_2 - T_s) + \Gamma(\dot{m}_1)^n = \frac{\dot{Q}_2 d}{k_eA} \qquad (18)$$

where, $\Gamma = \frac{CNd(\Delta T)}{2k_eA}A_p$ can be treated as a constant which is determined in terms of the subcooler design parameters, and fluid properties of the subcooler coolant.

Testing Procedure

The purpose of the test program was to evaluate the transient characteristics of the test CPL system by determining time variation of the evaporator temperature at several power inputs and inlet subcooling rates. Following the appropriate system preparation, approximately 0.85 liter of distilled and deggased water was introduced into the test system from the the fill reservoir. Then preliminary start-up tests were conducted in order to confirm normal CPL operation. Because of the design limitation of the existing test system, it was not possible to load all four evaporators at the same time following the system start-up. Therefore, tests were conducted by applying the step power input to only one evaporator at a time and keeping others at low power input of 50 watts per evaporator.

Step power input to a selected evaporator was varied between 50 to 300 watts. Time variation of evaporator temperature was recorded at several power input and inlet subcooling combinations. Except at very low subcooling rates, evaporators reached the steady states at power inputs used in this investigation.

Results and Conclusions

1. Transient Temperature Response

Figures 6 and 7 show evaporator heating surface temperature $T_e - T_o$ versus time τ obtained from experimental data. This data was collected at power inputs of 200 W and 300 W. At each power input, temperatures were recorded at two coolant flow rates of the evaporator inlet subcooler; 0.3 and 0.7 liter/min. Liquid entering the inlet subcooler was at the evaporator saturation temperature T_s.

Solid lines in these figures, going through the test data points, represent the temperature variations obtained by using Eq. (9). Referring to the curve in Fig. 6 for 0.3 liter/min. flow, for instance, β value from the test data was obtained as 0.0058 sec^{-1} whereas, the same value is predicted from the expression given for β if the power input $\dot{Q}_2$ is taken as 200 W instead of 300 W. It has been noted earlier that despite the use of insulation, evaporators of the present test system suffered significant heat losses. Therefore, it is reasonable to assume that only about 200 W of the 300 W power input contributed to vaporization in the evaporator.

Transient temperature test data of Figs. 6 and 7 show an exponential approach to equilibrium conditions. This is the characteristic of the quasi-steady state CPL performance represented by Eq. (8) which was obtained by using a lumped-heat-capacity model of the test CPL system.

Equations (8) and (9), however, deviate from

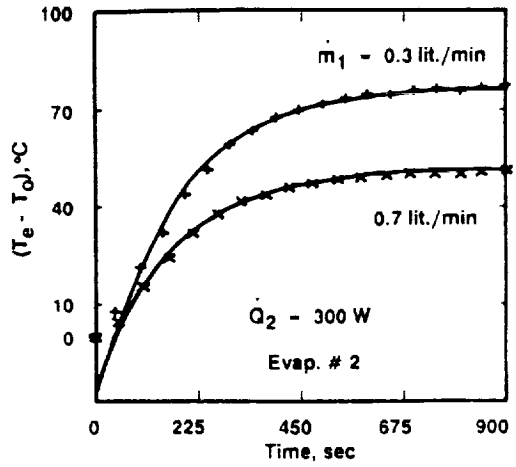

Fig. 6 - Variation of ($T_e - T_o$) vs Time, $\dot{Q}_2$ = 300 W

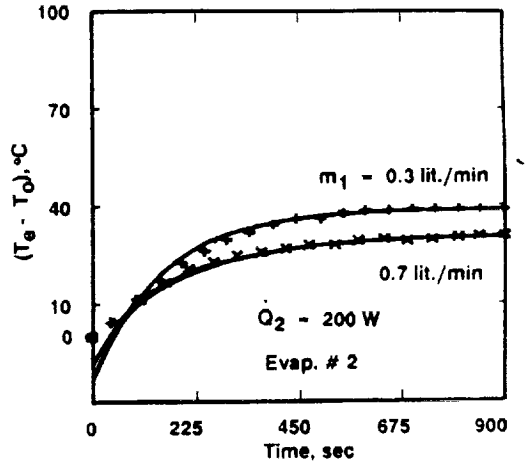

Fig. 7 - Variation of ($T_e - T_o$) vs Time, $\dot{Q}_2$ = 200 W

the experimentally determined temperature variations during the first 65 seconds after the pulsed power input is applied. This is caused by the thermal lag arising from the electric resistance heater which cannot provide the step power input to the evaporator instantly. Consequently, temperature response given by Eq. (9) has been modified by using a delay parameter τ_o in this equation,

$$T_e - T_o = \left(T_2 - T_o\right)\left[1 - e^{-\beta(\tau - \tau_o)}\right] \qquad (19)$$

This equation is used for $\tau > 65$ seconds. For $\tau \leq 65$ sec., a linear variation can be utilized. During the present experiments value of β was found to vary from 0.005 sec^{-1} to 0.0063 sec^{-1}, and the average value of τ_o was determined to be about 35 seconds.

It was evident that with proper inlet subcooling the test CPL system could achieve normal operation after suddenly applied heat load

However, when the subcooler coolant flow rate was decreased below 0.2 liter/min., evaporator dryout occurred even at low power inputs. Under dryout conditions, the capillary wick started drying out from the outer edges. Test data also indicated that evaporator wall temperature had a gradient in the radial direction which increased with decreasing inlet subcooling. Nevertheless, transient temperature response to a step power input has been found to satisfy the exponential form given by Eq. (8) at any location in the radial direction. Test data shown in Figs. 6 and 7 are given for temperature readings recorded with a single thermocouple attached to the evaporator surface.

The test system design did not allow changing of the reservoir temperature significantly. Therefore, tests were conducted at a single reservoir reference temperature, 30 deg. C.

2. Inlet Subcooling Effects

Experimental data of the present investigation has indicated a significant influence of the inlet subcooling on the evaporator temperature variation. In test runs with low inlet subcooling, evaporator dryout occurred even at very low power inputs. Visual observation of the evaporator capillary wicks indicated, even under normal operating conditions, varying degrees of partial dryout at outer edges of the capillary wicks. Extent of the dryout was proportional to the applied power, as well as the level of inlet subcooling.

Figure 8 shows variation of the steady state evaporator wall temperature (T_2-T_s) obtained from experimental data versus the inlet subcooler coolant flow rate at two different power inputs. In order to compare variation of the test data with the results predicted from Eq. (18), the coolant flow rate was expressed as $(\dot{m}_1)^n$. Solid lines in Fig. 8 represents the temperature variations predicted using Eq. (18). Although value of the constant (Γ) could be determined theoretically by using the given relationship, in view of the available test data, accuracy of this prediction would be questionable. Therefore, value of (Γ) was determined as a result of correlating the experimental data by using Eq. (18). Value of the exponential (n) in this equation is given in the literature in terms of Reynolds number.[4] The experimental value of the inlet subcooler Reynolds number in the present study varied between about 200 to 500. Value of (n) in this Reynolds number range can be taken as 0.385.

It is evident from Fig. 8 that Eq. (18) explains, at least qualitatively, effect of subcooling on the CPL evaporator surface temperature.

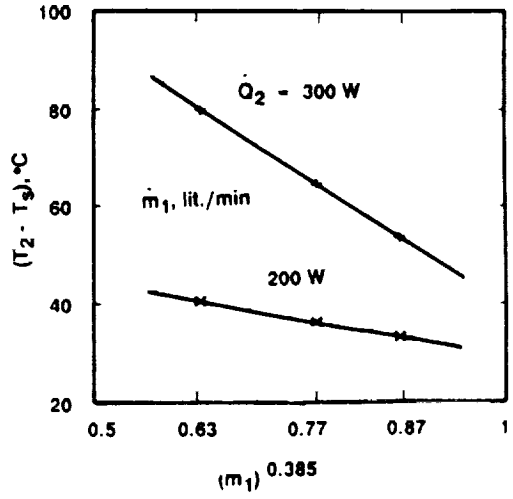

Fig. 8 - Variation of ($T_2 - T_s$) with inlet subcooling

Conclusions

It was evident that the experimental bench-top CPL system could achieve normal operation after a suddenly applied heat load. Test runs have indicated a significant influence of the inlet subcooling on the CPL performance. In test runs with low inlet subcooling evaporator dryout occurred even at low power inputs.

The lumped-heat-capacity CPL model developed in this study allows prediction of the transient response of the CPL test system. Good agreement has been obtained between the predicted and the measured temperature data. It is believed that the bench-top CPL test system and the model developed for this system can be used to investigate qualitatively transient characteristics of more elaborate CPL systems. In this sense, such research efforts supplement the more detailed quantitative information obtained by using the available computer programs that model the Capillary Pumped Loop heat pipe systems.

Acknowledgements

This study was supported by the Goddard Space Flight Center, National Aeronautics and Space Administration, under Research Grant No. NAG 5-834, and the support is gratefully acknowledged.

References

1. McCabe, Jr., M.E., Ku, J. and Benner, S., "Design and Testing of a High Power Spacecraft Thermal Management System", NASA Technical Memorandum 4051, June 1988.

2. Schweickart, R.B., Neiswanger, L. and Ku, J., "Verification of an Analytic Modeler for Capillary Pump Loop Thermal Control Systems", AIAA-87-1630, AIAA 22nd Thermophysics Conference, Honolulu, Hawai, June 1987.

3. Dynatherm Corporation, "Final Report for Capillary Heat Transport Systems", DTM-0218-1101, Prepared for National Aeronautics and Space Administration, Goddard Space Flight Center, October 1985.

4. Holman, J.P., Heat Transfer, Seventh Edition, McGraw-Hill, 1990.